PHILOSOPHICAL TRANSACTIONS A

rsta.royalsocietypublishing.org

Review

**Cite this article:** Garcia J, Liu SZ, Louie AY. 2017 Biological effects of MRI contrast agents: gadolinium retention, potential mechanisms and a role for phosphorus. *Phil. Trans. R. Soc. A* **375**: 20170180.
http://dx.doi.org/10.1098/rsta.2017.0180

Accepted: 30 August 2017

One contribution of 10 to a discussion meeting issue 'Challenges for chemistry in molecular imaging'.

**Subject Areas:**
chemical biology, inorganic chemistry, organometallic chemistry

**Keywords:**
nephrogenic systemic fibrosis, gadolinium in the brain, gadolinium toxicity, magnetic resonance imaging, contrast agents, gadolinium accumulation

**Author for correspondence:**
Angelique Y. Louie
e-mail: aylouie@ucdavis.edu

# Biological effects of MRI contrast agents: gadolinium retention, potential mechanisms and a role for phosphorus

Joel Garcia, Stephen Z. Liu and Angelique Y. Louie

Department of Biomedical Engineering, University of California, Davis, CA 95616, USA

AYL, 0000-0001-6610-5356

No discussion of challenges for chemistry in molecular imaging would be complete without addressing the elephant in the room—which is that the purest of chemical compounds needs to interact with a biological system in a manner that does not perturb normal biology while still providing efficacious feedback to assist in diagnosis of disease. In the past decade, magnetic resonance imaging (MRI) agents long considered inert have produced adverse effects in certain patient populations under certain treatment regimens. More recently, inert blood pool agents have been found to deposit in the brain. Release of free metal is often suspected as the culprit but that hypothesis has yet to be validated. In addition, even innocuous agents can cause painful side effects during injection in some patients. In this brief review, we summarize known biological effects for gadolinium- and iron-based MRI contrast agents, and discuss some of the potential mechanisms for the observed biological effects, including the potential role of phosphorus imbalance, related to kidney disease or cancer, in destabilizing gadolinium-based chelates and precipitating free gadolinium.

This article is part of the themed issue 'Challenges for chemistry in molecular imaging'.

## 1. Introduction

Contrast-enhanced magnetic resonance imaging (MRI) has been used widely for clinical and preclinical research, and it is estimated that more than 200 million



THE ROYAL SOCIETY PUBLISHING

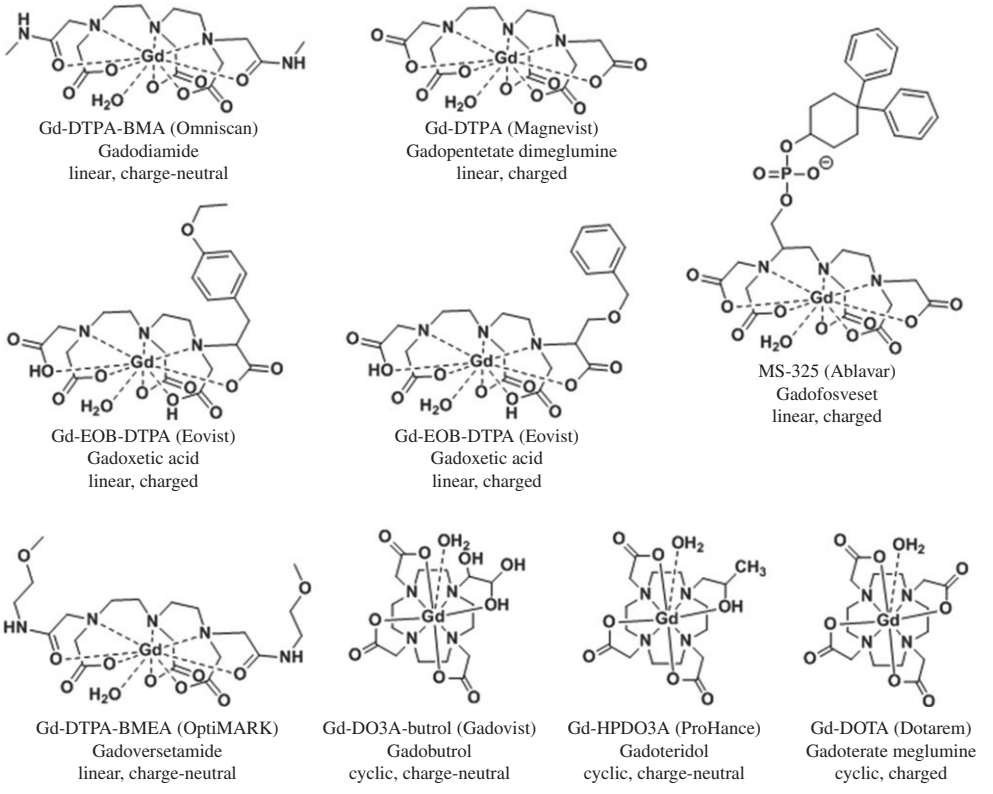


**Chart 1.** Chemical structures and chemical identification of gadolinium-based contrast agents.

doses of gadolinium-based contrast agents (GBCAs) have been administered worldwide [1]. Clinically used contrast agents have been based on gadolinium, manganese or iron oxide nanoparticles. However, several superparamagnetic, iron oxide nanoparticle agents have been discontinued due to lack of clinical use in imaging (Ferumoxytol is still in use for treatment of iron deficiency). Currently available agents are primarily gadolinium-based and, as recently as 2013, a new GBCA, gadoterate meglumine (Guerbet) was approved by the US Food and Drug Administration (FDA), making it the seventh FDA approved agent for MRI of the central nervous system (CNS) [2]. GBCAs (chart 1) were long considered safe until nephrogenic systemic fibrosis (NSF) was linked to GBCA administration in patients with renal impairment. Recently, there have been reports of gadolinium accumulating in brain tissues (table 1). The purpose of this brief review is to provide information about the observations of gadolinium toxicity and offsite activity, the potential mechanisms for gadolinium retention and the impacts of these biological effects on contrast agent design.

Because of its unique magnetic properties, the gadolinium ion has been widely used in the development of MRI contrast agents. A free gadolinium ion can accommodate up to nine water molecules to saturate its inner coordination sphere, which translates to very high contrast-enhancing efficiency (relaxivity). However, application of a free gadolinium ion as a contrast agent *in vivo* is limited because of its toxicity ($LD_{50}$ $GdCl_3{\cdot}6H_2O$: 100–200 mg $kg^{-1}$, IV in mice) [35] to biological systems. This lanthanide ion can readily precipitate with endogenous anions such as hydroxides, carbonates and phosphates. Carbonate and hydroxide salts of this metal may elicit expression of TGF-β in inflammatory cells and have been reported to stimulate fibroblast proliferation [36,37]. The similar ionic radius of $Gd^{3+}$ (107.8 pm) and $Ca^{2+}$ (114 pm) [38] means that trivalent gadolinium ions can compete with divalent calcium with higher affinity for $Ca^{2+}$-binding enzymes at nano- to micromolar concentrations, leading to adverse biological

**Table 1.** Reported NSF and brain hyperintensity and accumulation cases of clinically available GBCAs.

| | number of NSF reports [3] | | number of cases of brain hyperintensity on MRI (notes) [ref.] | | number of cases of Gd accumulation in the brain, quantitative (notes) [ref.] | |
|---|---|---|---|---|---|---|
| generic name (trade name) | unconfounded | confounded[a] | unconfounded | confounded[b] | unconfounded | confounded[b] |
| ***Linear*** | | | | | | |
| Gadodiamide (Omniscan) | 438 | 90 | yes, 61 [4–7]<br>8 (yes for 6 scans, no for 1–5 scans) [8] | yes, 36 (or gadopentetate) [9,10]<br>38 (at least 6 exposures) [11]<br>21 (absolute number of scans could not be confirmed) [12]<br>33 [13–15] | yes, 11 [16] | |
| Gadopentetate dimeglumine (Magnevist) | 135 | 276 | yes, 153 [13,17–21]<br>113 (all subjects received brain irradiation) [22] | yes, 32 (or gadodiamide) [9,14]<br>21 (other linear GBCAs) [12]<br>20 [10,13,23] | not evaluated | |
| Gadoversetamide (OptiMARK) | 7 | 11 | not evaluated | | not evaluated | |
| Gadobenate dimeglumine (MultiHance) | 0 | 8 | no, 140 [5,15,24] | yes, 18 (also with gadodiamide) [15] | yes, 15 [16] | |
| Gadoxetate (Eovist) | 0 | 0 | no, 33 (the administered dose was only a quarter of the amount of gadolinium as those with gadodiamide) [6] | | | 1 possibly confounded (non-statistical sample size, low-level Gd also detected in the uninjected patients) [25] |
| Gadofosveset (Ablavar) | 0 | 0 | not evaluated | | not evaluated | |

(*Continued*.)

**Table 1.** (*Continued*.)

| | number of NSF reports [3] | | number of cases of brain hyperintensity on MRI (notes) [ref.] | | number of cases of Gd accumulation in the brain, quantitative (notes) [ref.] | |
|---|---|---|---|---|---|---|
| generic name (trade name) | unconfounded | confounded[a] | unconfounded | confounded[b] | unconfounded | confounded[b] |
| ***Cyclic*** | | | | | | |
| Gadobutrol (Gadovist) | 1 | 2 | no, 296 [19,26] | yes, 58 possibly confounded [27]; see challenge by [28] and [29] | | yes, 2 possibly confounded (non-statistical sample size, low-level Gd also detected in the uninjected patients) [25] |
| Gadoteridol (ProHance) | 1 | 13 | | yes, 1 [23] | | yes, 2 [13]<br>5 possibly confounded (non-statistical sample size, low-level Gd also detected in the uninjected patients) [25] |
| Gadoteric acid (Dotarem) | 1 | 11 | no, 154 [30]<br>[18,31,32] | yes, 6 (exposed to linear GBCA) [10]<br>51 [23,33] | not evaluated | |

[a] A case is said to be confounded if two different GBCAs have been injected into a patient within eight weeks or longer [34].
[b] Use of other types of GBCAs could not be ruled out with certainty.

effects [39]. To minimize, if not prevent, gadolinium toxicity, one has to limit the access of free gadolinium to biological media. Chelating the gadolinium ion using multidentate organic ligands significantly reduces the interaction of the metal ion with the biological system, thereby dramatically decreasing the associated risk for gadolinium toxicity.

Clinically approved GBCAs feature gadolinium ions chelated with either macrocyclic or linear multidentate ligands to form charged or charge-neutral complexes. The potential to exhibit toxicity *in vivo* upon administration of GBCAs depends, in part, on the stability of the imaging agent itself. The stability of the gadolinium-based complex can be described by two independent parameters: thermodynamic stability and kinetic inertness. Both parameters are influenced by the ligand structure, and therefore can be manipulated using coordination chemistry principles such as hard–soft, acid–base, size match (for macrocyclic complexes) of the metal ion and macrocyclic cavity, and steric hindrance [40]. Reported conditional stability constants, defined as thermodynamic stability at physiological pH (log $K_{\text{eff}}$), for currently approved GBCAs range from 14.9 to 19, with macrocyclic $Gd^{3+}$-containing complexes having higher stability values over linear complexes, and charged complexes being more stable than charge-neutral complexes [38]. In biological systems, possible competitive chelation with endogenous ions such as zinc, calcium, iron and copper may also influence the stability of a gadolinium-containing complex because of the high affinity of these ions to organic ligands [41]. Competition with these biologically relevant ions can lead to dechelation of gadolinium from the complex and subsequent transmetallation. Dechelation and the relative thermodynamic and kinetic stability of GBCA have been prominent topics of discussion in the past decade with the high-profile observations of biological effects of gadolinium in NSF and in long-term retention in the brain.

## 2. Old news: nephrogenic systemic fibrosis

While NSF had been observed in renally compromised patients since the late 1990s, it was not until 2006 that correlations between NSF and GBCA were reported that profoundly impacted the MRI field. It was eventually determined that repeated administration of linear GBCAs to patients with renal insufficiency triggered development of NSF. This discovery prompted intense scrutiny with respect to the stability and toxicity profile of the clinically approved GBCAs, and led to modification of the existing safety guidelines governing the administration of linear contrast agents. The history of NSF and GBCA is well documented and thus only briefly summarized here [42,43]. Table 1 (adapted from a European Medical Agencies report, EMA/740640/2010) summarizes the number of accounts of NSF and the type of associated GBCA that was injected.

In a study by Frenzel *et al.* [44], the *in vitro* stability of commercially available GBCAs was assessed by incubating the imaging agents in human serum from healthy volunteers for 15 days. The rate of gadolinium release, quantified using high-performance liquid chromatography–inductively coupled plasma mass spectrometry (HPLC-ICP-MS), was highest for charge-neutral, linear GBCAs (20–21% released $Gd^{3+}$) followed by charged, linear GBCAs (0.07–1.9% released $Gd^{3+}$), while negligible amounts of free gadolinium were released by macrocyclic GBCAs. Subsequent animal experiments confirmed the higher potential of the charge-neutral, linear GBCAs to trigger gadolinium release that could induce NSF-like symptoms compared to macrocyclic GBCAs. Sieber *et al*. [45] used inductively coupled plasma atomic emission spectroscopy (ICP-AES) to determine the amount of gadolinium found in the skin of rats that received GBCAs. The obtained gadolinium concentration was 30-fold higher for rats that received the linear GBCA Omniscan compared to those rats that were treated with macrocyclic GBCAs Gadovist and Dotarem. Formation of NSF-like skin lesion was only observed in the skin of rats that received Omniscan [45]. The findings from the *in vitro* kinetic stability of GBCAs and animal studies indicate that the risk of developing NSF upon GBCA treatment can be correlated to the stability of the contrast agents against gadolinium release, with linear, charge-neutral GBCAs having a higher propensity to liberate gadolinium from the gadolinium complex relative to macrocyclic GBCAs.

In a separate paper by Sieber *et al.* [46], electron microscopic images of the dermis in some Omniscan-treated rats with NSF-like symptoms showed small gadolinium-containing particles that are deposited in macrophage-like cells. The high phosphorus concentration of these deposits may indicate that some of the gadolinium was deposited as $GdPO_3$. Abraham *et al.* [47] used scanning electron microscopy/energy dispersive X-ray spectroscopy (SEM/EDS) to examine the elemental composition, relative concentration and spatial distribution of tissue biopsies from gadodiamide-treated NSF patients and a gadodiamide-exposed but NSF-negative patient. The insoluble deposits obtained from the tissues contained gadolinium that was associated with phosphorus and calcium as detected in EDS. While ICP-AES and EDS cannot determine whether the gadolinium measured is in a free or chelated form, extended X-ray absorption fine structure (EXAFS) spectroscopy can probe local structure such as the type, position and number of neighbouring atoms. George *et al.* [48] used EXAFS to analyse gadolinium-containing deposits in autopsy tissue samples that were obtained from NSF patients. The difference between the EXAFS spectrum (figure 1) obtained from the insoluble deposit compared to that of GBCAs indicates that the gadolinium in the deposits may no longer be chelated. As illustrated in figure 1, Gd–P (3.11 Å) and Gd–Gd (4.05 Å) distances point to a $GdPO_4$ structure (curves 1), supporting the earlier notion of gadolinium ion depositing in the form of insoluble $GdPO_4$. These peaks are not present in the GBCA spectra (curves 2 and 3).

Several studies [36,43,49,50] have been made exploring the mechanism of gadolinium release from GBCAs to understand the role of the free gadolinium ion in NSF pathophysiology. These studies implicated acidosis, transmetallation by endogenous ions and protein binding as possible means for gadolinium release from GBCAs. Grobner *et al.* [36] reported that end-stage renal disease patients who developed NSF-like symptoms had acidosis (serum pH of less than 7.35) at the time of using Omniscan, while no acidosis was observed for healthy patients. A combination of acidosis and extended residence time of administered GBCAs *in vivo* may favour dissociation of gadolinium from the linear gadolinium complex, which can also be facilitated by endogenous metals such as zinc, copper, iron and calcium [36]. A study by Rowe *et al.* [49] demonstrated the binding of GBCAs by the acidic serine aspartate-rich MEPE-associated (ASARM) peptides *in vivo*. The acidic character of ASARM peptides was hypothesized to induce gadolinium release from GBCAs, increasing the risk of NSF. This hypothesis was tested *in vitro* by measuring the dissociation of gadolinium ion when Omniscan was exposed to ASARM peptides and an ASARM-binding peptide, SPR4. Using HPLC linked to LC-ICP-MS, the ratio of free and bound gadolinium from a mixture of Omniscan and ASARM peptides was determined to be significantly higher compared to when SPR4 is present in the mixture of Omniscan and ASARM. The observed ASARM–gadodiamide peak in HPLC confirmed the interaction of the peptide with gadodiamide. These data support that ASARM peptides can induce the release of gadolinium from GBCA. To explore the role of ASARM peptides in developing NSF-like pathology *in vivo*, a murine model of X-linked hypophosphatemic rickets (Hyp) with elevated ASARM peptides in the circulation and bone was treated with MultiHance. An increase in phosphate and calcium levels in serum was observed for mice infused with MultiHance alone, while no change in phosphate and calcium levels in serum was noted when mice were treated with MultiHance and SPR4. Although their animal studies require further investigation, the obtained data suggest that the ASARM-induced gadolinium release from GBCA may cause displacement of calcium and phosphate from the bone, leading to increased levels of phosphate and calcium in mice serum.

The current model of gadolinium-induced NSF purports the process to be initiated by CD34+ fibroblasts [38,43,51]. These fibroblasts mature and take on the phenotype of spindle cells, leading to faulty scar formation [43]. The cause of stimulation of fibrogenic changes may not only be limited to free gadolinium ions that are released from GBCAs, but also include several forms of gadolinium (i.e. salts, free and chelated). *In vitro* studies by Bleavins *et al.* [37] demonstrated that both chelated gadolinium (Omniscan and Magnevist) and insoluble phosphates and carbonates of gadolinium were capable of stimulating fibroblast proliferation in a manner that was dose-dependent. The findings in this study indicate that dechelation of gadolinium from GBCAs may not be necessary for fibrosis to occur and open another area of research aiming to better

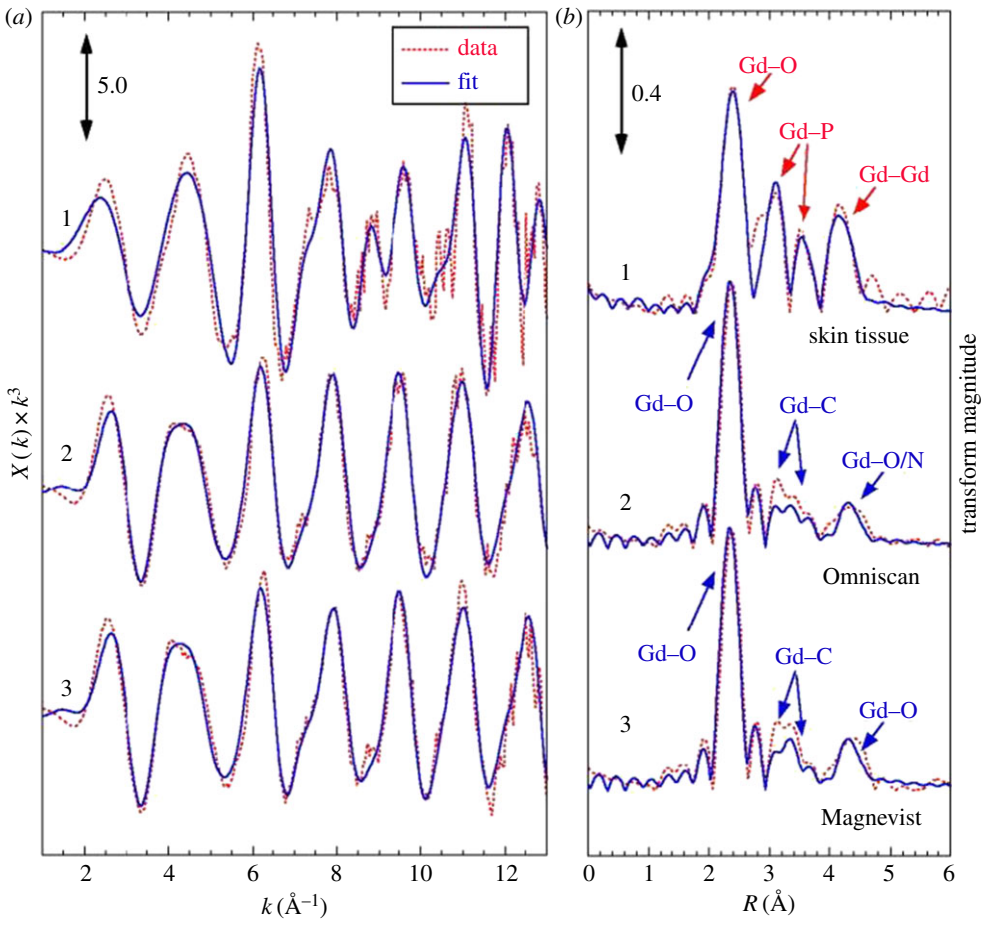


**Figure 1.** Extended X-ray absorption fine structure (EXAFS) spectra at the Gd $L_3$-edge and analysis of the tissue sample compared to selected GBCAs. (*a*) EXAFS spectra and (*b*) Fourier transforms with simulated fits of (1) skin tissue, (2) Omniscan and (3) Magnevist. The Fourier transforms are phase-corrected assuming Gd–O interactions. Indicated are the atomic origins of the observed peaks. These data suggest that the deposited gadolinium is no longer in chelated form and may exist predominantly as an insoluble gadolinium phosphate. Adapted from [48]. (Online version in colour.)

understand the pathophysiologic changes underlying GBCA-induced NSF and other fibrotic diseases. As a result of the studies mentioned here and many others, an understanding of the relation between GBCA structure and NSF was reached, and new guidelines were enacted for patient treatment, discouraging the use of linear GBCAs in patients with renal insufficiency, which has nearly eliminated the incidence of NSF.

## 3. Recent news: hyperintensity and gadolinium in the brain

### (a) Early observations of gadolinium accumulation

Just as the furore over NSF abated, evidence that gadolinium accumulates in the brain resurfaced. The retention of gadolinium after GBCA injection in bone has been known for some time, and reported in a number of studies on animals and bone samples from patients who had received GBCAs prior to hip replacement surgery [52–55]. Higher gadolinium values were found for linear chelates than for macrocycles, suggesting some connection to the kinetic lability of the GBCAs; moreover, these were patients receiving a standard dose of GBCAs with normal renal function.

However, long-term retention in the brain was a curious and unexpected finding, as GBCAs have been used for decades to diagnose blood–brain barrier (BBB) permeability, due to their inability to cross an intact BBB [56]. Gadolinium chloride studies in animals do not find histological changes in the CNS, leading to the belief that free gadolinium also does not cross the BBB to any pathological extent [57,58]. Particularly troublesome was that some of the GBCA observations have been made in patients with normal renal function. An early 2010 retrospective study found gadolinium phosphate deposits in a limited number of brain tumour biopsies from patients with normal renal function [16]. Thirty biopsies from 28 patients were collected, and gadolinium deposits were found in seven biopsies from five patients. Greater deposition was found in Omniscan-treated patients than in those treated after the institution switched to MultiHance in 2007. The deposits tended to be in highly vascular areas and often found associated with calcified regions in vessel walls. Interestingly, the insoluble deposits found were similar in elemental composition to those found in tissues of patients with renal disease. The studies were performed with SEM/EDS, which cannot distinguish whether the deposited gadolinium is in complexed or unchelated form. Gadolinium at neutral pH would rapidly form insoluble gadolinium hydroxide colloids [58]. It is possible, then, that gadolinium exists either in precipitates or as chelated gadolinium that is adsorbed on the tissue [16]. This is not without precedent; for example, adsorption of chelated lanthanides onto hydroxyapatite has been observed in highly charged lanthanide complexes of 1,4,7,10-tetraazacyclododecane-1,4,7,10-tetrakis(methylenephosphonic acid) ($H_8$DOTP) such as $^{153}SmDOTP^{5-}$ and $^{111}InDOTP^{5-}$ [59].

In 2011, a case report from a renally compromised NSF patient who had received multiple injections of Omniscan found insoluble gadolinium phosphate deposits in multiple tissues. These authors also used SEM/EDS. Similar to the results of the study above, the authors found gadolinium deposition to be primarily vascular in nature, in vessel walls, but also in brain parenchyma [60]. This was one of the first reports to observe gadolinium accumulation outside of the skin for an NSF patient. The vessel walls are also sites for calcium deposition in renal failure, and a similar mechanism could be at work for gadolinium. The calcium phosphate imbalance in chronic renal failure patients is cited as a risk factor for developing NSF with GBCA injection. However, this does not explain the similar deposits found in patients with normal renal function. The method by which the insoluble phosphates form is unresolved. Gadolinium could be released by the chelate and precipitate with surrounding co-ions, or it may directly associate with calcium deposits. Further study is necessary.

Possible compromise of the BBB has been cited as a potential reason for the accumulation observed in these early reports. The common occurrence of hyperintensity in the dentate nucleus and globus pallidus (GP) on unenhanced $T_1$-weighted MR images was previously associated with patients who had undergone brain irradiation, or who had multiple sclerosis and other diseases, and it was assumed this was an artefact of disease-related BBB permeability; thus, a causal relationship with contrast enhancement was not immediately suspected [9].

## (b) Clinical retrospective studies of past images: linear GBCAs correlate with hyperintensity in $T_1$ images in patients with normal renal function, but multiple GBCA injections

In the last few years a cluster of high-profile reports have elevated public concern by concluding that the accumulation of gadolinium in the brain, revealed as MRI hyperintensity in the dentate nucleus (DN) and GP, was correlated with multiple GBCA injections, even in patients with normal renal function [9]. In fact, a linear correlation was found between progressive hyperintensity in the DN-to-pons signal intensity ratio in unenhanced $T_1$-weighted images and the number of gadodiamide-enhanced MR imaging studies performed [11]. In one, perhaps extreme, example, for a survey of 179 121 contrast-enhanced MRI studies over 15 years, the authors found 33 brain tumour patients who had received 35 or more GBCA administrations, representing 550 different imaging studies [14]. Measuring images after 6, 12, 24 and the final GBCA administration, the authors found increasing $T_1$ signal intensity in the dentate nucleus, GP and red nucleus after six

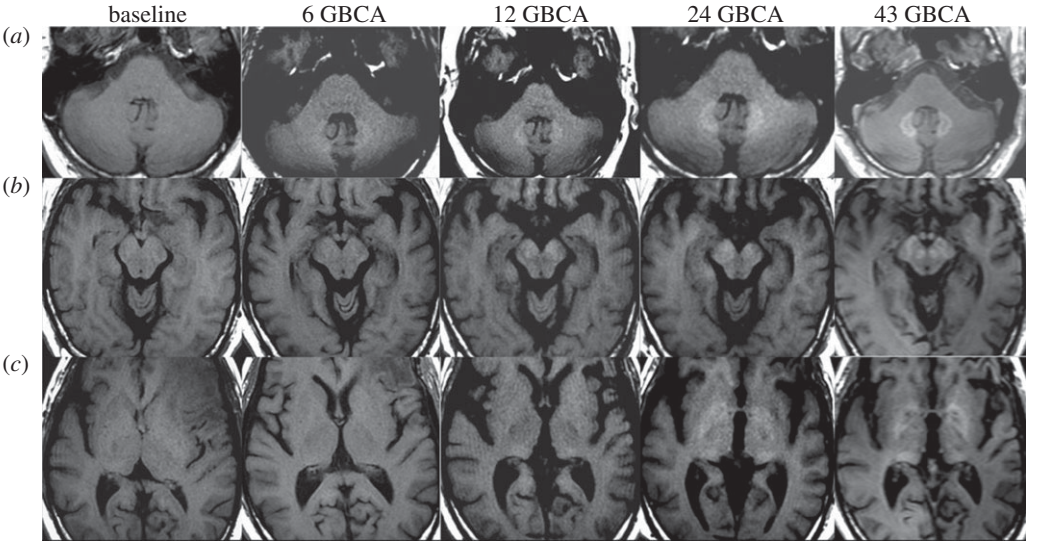


**Figure 2.** MR images in a 52-year-old man with left frontal glioblastoma. Dentate nucleus (*a*), cerebral peduncle, substantia nigra and red nucleus (*b*), and globus pallidus and posterior thalamus (*c*) all gradually increase unenhanced $T_1$ signal intensity after 43 linear GBCA administrations. Adapted from [14].

administrations. As the number of administrations increased, so did the number of brain regions showing hyperintensity. Several other regions in the brain, including the substantia nigra and posterior thalamus, began to show signal intensity changes with increasing numbers of GBCA administrations. This is illustrated in figure 2 showing images from a single patient over the course of the increasing number of GBCA administrations. Signal intensity increase was greatest for the dentate nucleus, which the authors [14] surmise is the reason that this region was the first to be noted to increase in signal with multiple GBCA injections. These and other reports support initial findings that demonstrate the association of hyperintensity with linear GBCAs, and a cumulative deposition with increasing numbers of administrations of linear agents the patient has received [5,61–63].

Taken together, the observed hyperintensity in some regions of the brain such as the dentate nucleus and GP is presumed to be associated with the gadolinium deposited in these regions after exposure to GBCA. While SEM/EDS data suggest that the gadolinium is possibly deposited as insoluble phosphate salt, it remains unclear whether all the deposited gadolinium is in this form or is a mixture of insoluble phosphate salts and chelated gadolinium. The reports generate many more questions than they answered. The data or metadata on patients were acquired non-invasively through imaging, and lacked quantitative information of exactly how much gadolinium is accumulated, and it is unclear if free gadolinium or gadolinium complexes were the signal-generating species. Gadolinium present in insoluble form is not expected to increase signal intensity on a $T_1$-weighted image, as gadolinium must be present in solution to effectively relax water protons. Gadolinium surface-bound to a calcium deposit could have coordination sites available for relaxivity, and repeat scans may repeatedly introduce gadolinium to the surface of the deposits over time. Alternatively, it is possible that the increase in signal intensity in some regions of the brain can be attributed to other soluble forms of gadolinium, which could be chelated and/or protein-bound gadolinium. Therefore, there is a need for biophysical techniques that can explore the speciation of GBCAs once administered in the body. X-ray fluorescence has already been used to map the chemical distribution of metals in all chemical forms in the cerebellum and therefore could be used for identifying the chemical form (e.g. oxidation state, whether protein-bound or free, whether intra- or extracellular) of metals in tissues [64]. Hydrophilic interactive liquid chromatography combined with ICP-MS measurement

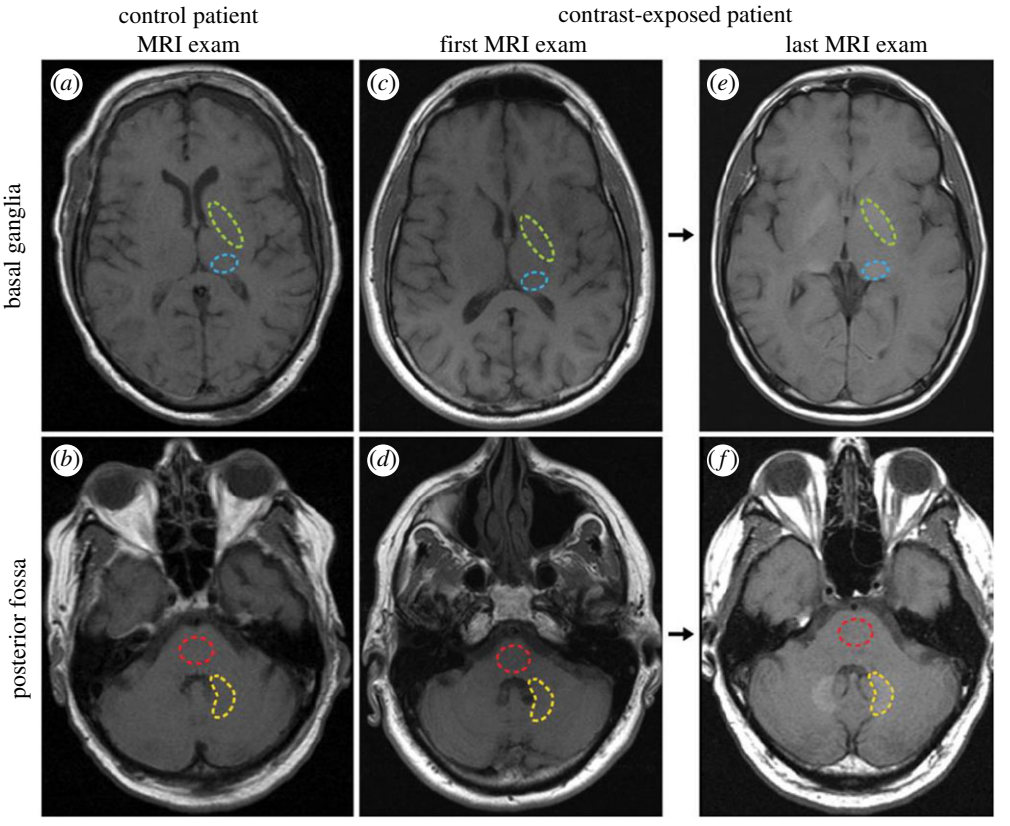


**Figure 3.** Axial $T_1$-weighted MR images through the (*a*,*c*,*e*) basal ganglia and (*b*,*d*,*f*) posterior fossa at the level of the dentate nucleus. Images are shown for (*a*,*b*) control group patient 4, and the (*c*,*d*) first and (*e*,*f*) last examinations performed in contrast group patient 13. Regions of interest used in the quantification of signal intensity are shown as dashed lines for the globus pallidus (green, upper region), thalamus (blue, lower region), dentate nucleus (yellow, lower region) and pons (red, upper region). Adapted from [4]. (Online version in colour.)

(HILIC-ICP-MS), which has been used to identify chelated ProHance in the skin of NSF patients, could be applied to determine the form of the gadolinium in tissues [65].

## (c) Quantitative evaluation of clinical autopsy samples: linear GBCAs correlate with gadolinium in tissues, which increases with more administrations

The imaging reports were subsequently followed by quantitative assays of autopsy tissues using methods such as ICP-MS to measure actual gadolinium levels in tissues. In one study, analysis of samples from the dentate nuclei, pons, GP and thalamus collected from 13 patients who had received at least four injections of gadodiamide, a linear chelate, were found to have 0.1–58.8 µg of gadolinium per gram of tissue, widespread throughout the brain. This is in comparison to undetectable levels of gadolinium in control patients [4]. Figure 3 gives an example of imaging data from a patient in this retrospective study, which illustrates the brain regions used for quantification of the signal intensity; a progressive increase in signal from the first exam to the last exam is evident in the dentate nuclei (yellow, lower dashed region) in figure 3*f* and GP (green, upper dashed region) in figure 3*e*. Transmission electron microscopy and X-ray microanalysis on these tissues found extensive gadolinium deposits in the brains of the patients receiving contrast. Similar to earlier work, gadolinium was found in vessels, in endothelial walls; however, unlike the earlier studies, densitometry suggested there was a sizeable, 18–48%, fraction of gadolinium in the

neural interstitium—implying that gadolinium had crossed the BBB. These images are presented in supplemental data for the McDonald paper [4]. In 0.2% lead citrate-stained samples, it is a bit easier to distinguish the high-density foci that the authors report as containing gadolinium. Identifying the gadolinium-containing deposits appears to be an arduous process, as there are other electron-dense foci that are gadolinium-free (an example containing only carbon, oxygen, caesium and osmium is shown in the control—the source of the Cs is a bit unclear, as it is not contained in the staining solution named in the material and methods section). There was no histological evidence of damage to the neural tissues in any subjects; this is in spite of some patients undergoing up to 29 MR examinations and receiving up to 500 ml of the linear agent gadodiamide (287 mg $ml^{-1}$). In another study, brain tissue was obtained at autopsy from 10 subjects with normal renal function, of whom five received linear GBCAs, while the other five were controls who did not receive contrast. Significant gadolinium content was found in all tissues for GBCA-treated subjects, and was higher in the dentate nucleus and GP (mean: 0.44 µg gadolinium $g^{-1}$ of tissue versus 0.12 µg gadolinium $g^{-1}$ in other regions) [13]. Although the absolute amount of gadolinium is still quite low here—much lower than the amount injected (0.1–0.3 mM $kg^{-1}$), much lower than the anticipated exposure experienced by the kidney during clearance and far lower than the $LD_{50}$ for $GdCl_3$ of 100–200 mg $kg^{-1}$ [66]—it is the long-term persistence of gadolinium in the brain that presents the dilemma. The number of subjects in these studies is small, but the involvement of linear chelate GBCAs in potentially dangerous side effects triggered some alarm after the fresh memory of the NSF tragedies.

Although no deleterious health effects have been observed to date, government regulatory bodies worldwide are exercising caution and some already are instigating preventative measures to minimize risk from linear agents. The FDA released a safety announcement in July 2015 that they were 'investigating the risk of brain deposits following repeated use of gadolinium-based contrast agents (GBCAs) for magnetic resonance imaging (MRI)', although they state that 'it is unknown whether these gadolinium deposits are harmful or can lead to adverse health effects'. In the safety announcement, the FDA also urged medical professionals to weigh the benefits for the information that could be provided against the accumulation of gadolinium that occurs with repeated injection of GBCA and its potential risk. The FDA posted an update on 22 May 2017 that it had not found any adverse health effects from GBCA retention in the brain and, therefore, did not feel a need to restrict GBCA use at this time. The European Medicines Agency (EMA), on the other hand, just a few months ago, in March 2017, recommended suspension of the marketing authorizations for four linear gadolinium contrast agents due to 'convincing evidence of accumulation of gadolinium in the brain . . . many months after the last injection of a gadolinium contrast agent', but also noted that 'no symptoms or diseases linked to gadolinium in the brain have been reported'. Patient safety is paramount, and the long-term effects of low-level accumulation has not been determined yet; more meta-analyses are required to tease out if there is any increase in risk of neurological complications due to the presence of lanthanide in the brain.

## (d) Not clear if macrocyclic GBCAs form deposits or cause hyperintensity

Whether administration of macrocyclic chelates produces similar hyperintensity or gadolinium accumulation is still unclear and the literature is contradictory and at times controversial. Several reports find no evidence of hyperintensity for patients receiving macrocyclic chelates [67]. But one study, using ICP-MS on tissues from nine autopsy cases (out of 134) who had received one or more doses of only one type of contrast (gadoteridol, gadobutrol, gadobenate or gadoxetate) agent, found gadolinium in brain and bone from patients injected with macrocyclic GBCA, with higher deposition in bone [25]. It was noted that the levels of gadolinium were several-fold lower for tissue from patients injected with macrocyclic agents compared to those injected with linear agents (20 times lower for ProHance than for Omniscan) and the actual amount of gadolinium deposited was very small, of the order of a few ng $g^{-1}$ of tissue. Still, the pattern of higher amounts of gadolinium from linear chelates would be consistent with the hypothesis of transmetallation or dechelation of the GBCA over time.

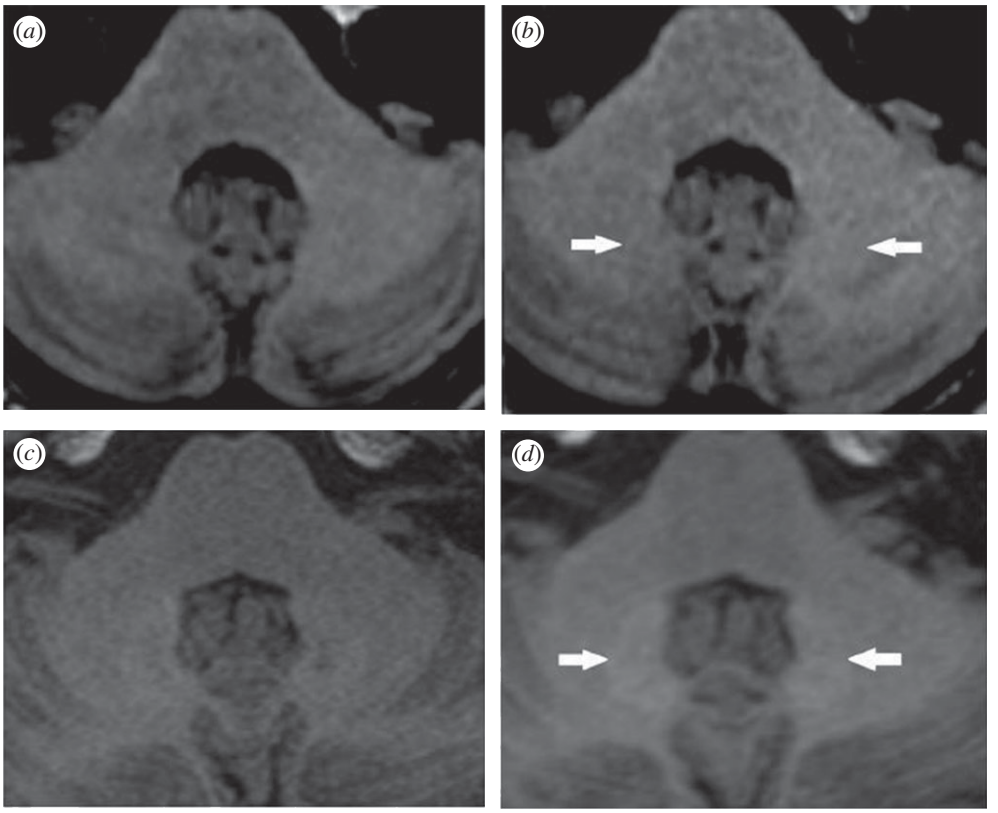


**Figure 4.** Unenhanced $T_1$-weighted MR brain images that were acquired before (*a*,*c*) and after six administrations of macrocyclic GBCA, gadoterate meglumine, Dotarem (*b*), and linear GBCA, gadopentetate dimeglumine, Magnevist (*d*). The observed hyperintensity is apparent in the dentate nucleus (white arrows) of the subject who underwent repeated administration of linear GBCA. Adapted from [18].

On the other hand, a retrospective study, which was performed on two groups of 50 patients who underwent at least six administrations of exclusively linear gadopentetate dimeglumine (Magnevist) or macrocyclic gadoterate meglumine (Dotarem) as contrast agents, found no signal intensity difference for macrocyclic GBCA [18]. The selected patients had normal renal function (estimated glomerular filtration rate, eGFR $< 60\,\mathrm{ml\,min^{-1}\,m^{-2}}$) and did not have a history of brain haemorrhage, stroke, brain ischaemia, intracranial infections or lesions in the pons or cerebellum. The signal intensity of the dentate nucleus (DN) in an unenhanced $T_1$-weighted image was compared to that of the pons, cerebrospinal fluid (CSF) and cerebellum. The DN-to-pons signal intensity ratio was found to be 'significantly higher than 0' for the group that received linear GBCA as illustrated in figure 4, while no increase in the DN-to-pons signal intensity ratio was observed for the macrocyclic GBCA group. Another report of accumulation in patients receiving macrocyclic compounds has been criticized for its MR images, which did not show a difference in signal [67]. Additional evaluations with larger numbers of subjects and controlled consideration of confounding factors are required before a conclusion of risk from macrocyclic compounds can be drawn. A review by Radbruch in 2016 provides a helpful table (not shown here) that summarizes studies in humans up to 2016 and includes specific information about which linear and macrocyclic compounds were administered [67]. In table 1 we summarize the studies reviewed here that have evaluated gadolinium deposition in the human brain by imaging or other methods.

Why are the observations for macrocyclic agents inconsistent? The Murata study [25] uses highly sensitive ICP-MS and it is possible that the amounts of gadolinium present were

insufficient to yield contrast in MR images collected by Radbruch [67]. Although the individuals selected for the Murata study had undergone contrast-enhanced MRI, there was no inclusion or mention of the imaging results and whether hyperintensity was evident. Other possibilities for discrepancy could include measurement error; samples were obtained by sectioning and it is possible for some cross-contamination in ICP-MS. Disease-related factors could also have played a role in the differences observed. In the two examples above, the types of autopsy cases differed significantly—in the Murata paper, the decedents had a variety of different major diagnoses, and, except for two decedents with hepatocellular carcinoma, no two diagnoses were the same. The application of brain MRI suggests that there were brain metastases or co-morbidity with brain tumour. The authors also state that they could not be completely certain that other agents might have been administered which were not included in the records. In the Radbruch paper, most of the autopsy subjects were glioma (grade I–III) or glioblastoma patients who had a history of chemo- and radiation therapy. Could there be a difference in BBB permeability for primary versus metastatic brain disease? This is another possibility for the discrepancy in data.

There are several limitations to the studies in the literature. Most report data from a limited number of subjects. Often the amount of injected dose is not available; also, the image acquisition parameters vary by institutions, so it is difficult to compare between studies [68]. A significant limitation to sifting through the increasing number of reports is that the subjects selected from autopsy samples are primarily sorted by whether or not they received contrast, not by the pathology which called for the contrast study. Most of the subjects studied have been cancer patients, who were receiving MRI scans to monitor their disease, and it is still unclear whether the disease and its treatment may have compromised the BBB; thus, a pathologically influenced permeability to GBCA cannot be ruled out. Perhaps the key to unravelling this mystery lies in the normal volunteers who were part of phase I trials of GBCAs, but they may have not received multiple courses of contrast sufficient to observe deposits.

## (e) Studies in animal models, tumour-free and with/without normal renal function

More in-depth studies can be performed in animal models where subjects of specific disease or free of disease could be studied, dosing could be controlled and other tissue samples could be collected at specified time points for quantitative analysis. Historically, early animal studies on gadolinium toxicity observed mineral emboli in capillaries in both rats [58] and mice [57] after intravenous (IV) injection of $GdCl_3$. Thus, some of the human results are reminiscent of the effects of free gadolinium injection. Mineral deposition in mononuclear phagocytic cells was also observed after $GdCl_3$ injection to rats and mice, which was attributed to scavenging of gadolinium hydroxide colloids by these cells. Gadolinium chloride injection also resulted in hypotension. There were clear toxic effects for animal studies of gadolinium salts that have not been observed in humans or animals receiving GBCA injections. To date, the GBCAs do not seem to accumulate at high enough concentrations or in the correct form to exert toxicity in patients or research models. Many animal studies were performed in the wake of the NSF discovery, but these focused on the skin and clearance organs [69]. Today, increasing numbers of controlled studies of the brain in rat and mouse models are being performed in which GBCAs were administered to healthy animals and models of renal dysfunction. These animal studies provide valuable observation groups that have not been accessed for human patients. As noted earlier, healthy adult humans are unlikely to be injected with contrast unless they were volunteers for a clinical trial. In table 2, we summarize the animal studies reported to date that have studied the retention of gadolinium in the brain and CSF, and discuss them below.

Robert *et al.* [61] performed IV injections of 0.6 mmol $kg^{-1}$ gadoterate meglumine (macrocyclic, recommended human dose 0.3 mmol $kg^{-1}$) and gadodiamide (linear) GBCAs at four times a week over five weeks on $n = 7$ rats, which were then examined by brain $T_1$-weighted MRI, with subsequent collection of tissues for ICP-MS. Similar to the human results, hyperintensity was found in the deep cerebellar nuclei (DCN) for the linear chelates, which increased with eight or more injections and which persisted through the five weeks after the last injection. No effect

**Table 2.** Animal studies reported to date that have investigated the retention of gadolinium in the brain and CSF.

| reference | agent | injection protocol | amount | tissue/organ examined | method of analysis | major findings |
|---|---|---|---|---|---|---|
| Rasschaert [70] | 1. Gadodiamide | intravenous injection four times per week for five weeks | 0.6 mmol Gd $kg^{-1}$ body weight, daily injection | 1. Brain (DCN, CSF, parietal bone and cerebellum)<br>2. Plasma<br>3. Femur | 1. ICP-MS<br>2. $T_1$-weighted MRI | 1. Increased $T_1$ in deep cerebellar nuclei<br>2. Hypersignal in choroid plexus<br>3. Plasma Gd concentration at 1 µmol $l^{-1}$ |
| Jost [62] | 1. Gadodiamide<br>2. Gadopentetate dimeglumine<br>3. Gadobenate dimeglumine<br>4. Gadobutrol<br>5. Gadoterate meglumine | slow-hand intravenous injections<br>10 injections in total, each on five consecutive days per week | 2.5 mmol Gd $kg^{-1}$ body weight for the study of signal enhancement<br>1 mmol Gd $kg^{-1}$ body weight for the study of CSF space | 1. Brain | 1. Whole-brain MRI<br>2. MRC<br>3. FLAIR MRI | 1. Increased signal intensity in CN for linear GBCAs<br>2. No signal intensity change in CN or GP for macrocyclic GBCAs<br>3. Both GBCAs can pass the blood–CSF barrier |
| Jost [71] | 1. Gadopentetate dimeglumine<br>2. Gadodiamide<br>3. Gadobenate dimeglumine<br>4. Gadobutrol<br>5. Gadoterate meglumine<br>6. Gadoteridol<br>7. Gadomer (experimental) | one-time intravenous injection | 1.8 mmol Gd $kg^{-1}$ body weight | 1. Brain (cerebellum and pons)<br>2. Blood<br>3. CSF | 1. MRC<br>2. FLAIR MRI<br>3. ICP-MS | 1. No effect of GBCA structures on CSF penetration and distribution<br>2. Enhanced MRI signal in CSF<br>3. GBCA clearance within 24 h |

(*Continued*.)

**Table 2.** (*Continued*.)

| reference | agent | injection protocol | amount | tissue/organ examined | method of analysis | major findings |
|---|---|---|---|---|---|---|
| Smith [72] | 1. Gadodiamide | low-dose group: two doses per week for five weeks<br>high-dose group: four doses per week for five weeks | 0.6 mmol Gd $kg^{-1}$ body weight, daily dose | 1. Brain<br>2. Blood | 1. ICP-MS | 1. 0.00019% of injected dose after 1-week dose<br>2. 0.00011% of injected dose after 20 weeks |
| Kartamihardjia [73] | 1. Gd-DTPA-BMA<br>2. Gd-DOTA<br>3. $GdCl_3$ | intravenous injection on weekdays for four weeks | 1. Gd-DTPA-BMA: 5 mmol Gd $kg^{-1}$ body weight<br>2. Gd-DOTA: 5 mmol Gd $kg^{-1}$ body weight<br>3. $GdCl_3$: 0.02 mmol Gd $kg^{-1}$ body weight | 1. Liver<br>2. Bone<br>3. Spleen<br>4. Skin<br>5. Kidney | 1. ICP-MS | 1. Short-term Gd retention increased for Gd-DTPA-BMA<br>2. Long-term Gd retention increased for Gd-DOTA<br>3. Hepatic and splenic Gd retention increased for $GdCl_3$ |
| Robert [63] | 1. Gadobenate dimeglumine<br>2. Gadopentetate dimeglumine<br>3. Gadodiamide | eight rats per group received 20 intravenous injections for five weeks (four injections per week) | 0.6 mmol Gd $kg^{-1}$ body weight | 1. Plasma<br>2. Brain (dorsal cochlear nucleus) | 1. ICP-MS<br>2. $T_1$-weighted MRI | 1. Increased $T_1$ in DCN for linear GBCAs versus macrocyclic<br>2. Increased Gd concentration in the cerebellum for linear GBCAs |

(*Continued*.)

**Table 2.** (*Continued.*)

| reference | agent | injection protocol | amount | tissue/organ | method of analysis | major findings |
|---|---|---|---|---|---|---|
| Robert [61] | 1. Gadoterate meglumine<br>2. Gadodiamide | intravenous injections four times per week for five weeks | 0.6 mmol Gd $kg^{-1}$ body weight | 1. Plasma<br>2. Brain (DCN) | 1. ICP-MS<br>2. $T_1$-weighted MRI | 1. Persistent $T_1$ hyperintensity in DCN for gadodiamide<br>2. Gadolinium concentration higher in the cerebellum for gadodiamide |
| Spencer [58] | 1. $GdCl_3$ | one-time intravenous injection at four different dosages | 1. 0 (saline)<br>2. 0.07 mmol Gd $kg^{-1}$ body weight<br>3. 0.14 mmol Gd $kg^{-1}$ body weight<br>4. 0.35 mmol Gd $kg^{-1}$ body weight | 1. Kidney<br>2. Liver<br>3. Lung<br>4. Ovaries<br>5. Spleen<br>6. Testes<br>7. Thymus<br>8. Bone marrow<br>9. Heart<br>10. Stomach | 1. Blood content test<br>2. Necropsies<br>3. TEM<br>4. EDAX X-ray | 1. Mineral deposition in capillary beds<br>2. Phagocytosis of mineral<br>3. Hepatocellular and splenic necrosis<br>4. Dystrophic mineralization<br>5. Fundic glandular mucosa mineralization |
| Spencer [57] | 1. $GdCl_3$ | one-time intravenous injection at four different dosages | 1. 0 (saline)<br>2. 0.07 mmol Gd $kg^{-1}$ body weight<br>3. 0.14 mmol Gd $kg^{-1}$ body weight<br>4. 0.35 mmol Gd $kg^{-1}$ body weight | 1. Kidney<br>2. Liver<br>3. Lung<br>4. Ovaries<br>5. Spleen<br>6. Testes<br>7. Thymus<br>8. Heart<br>9. Stomach | 1. Blood content test<br>2. Necropsies | 1. Cholesterol and globulin raised<br>2. Histological lesions |

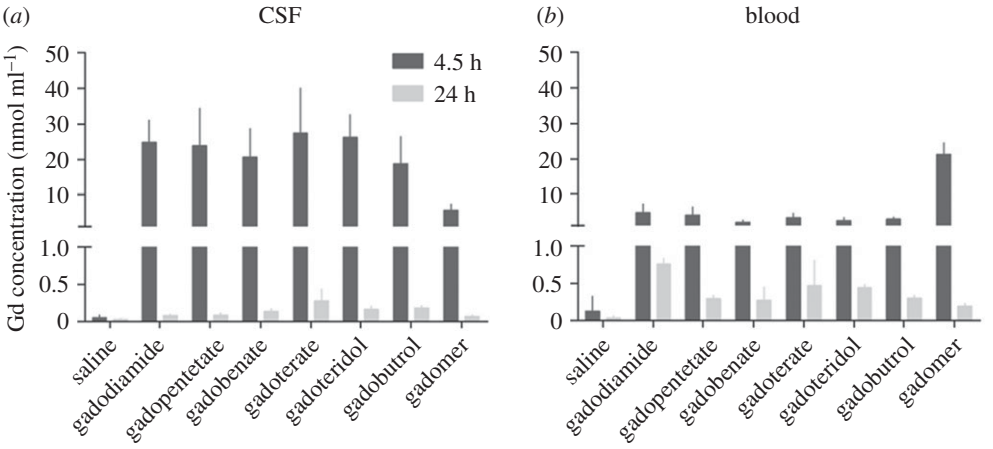


**Figure 5.** Gadolinium (Gd) concentrations in CSF and blood. The gadolinium concentration determined in the CSF (*a*) and blood (*b*) samples obtained at 4.5 h and 24 h, respectively. Gadopentetate, gadopentetate dimeglumine; gadobenate, gadobenate dimeglumine; gadoterate, gadoterate meglumine; error bars represent the standard deviation. Adapted from [62].

was seen for the macrocyclic GBCA [61]. These imaging data are shown in summary in figure 5. Gadolinium quantification by ICP-MS found concentrations eightfold to 52-fold higher in the brains of animals treated with linear chelates compared to animals exposed to macrocyclic GBCA or saline. The total gadolinium was reported higher in the cerebellum (3.66 nmol $g^{-1}$), cerebral cortex (2.32 nmol $g^{-1}$) and subcortical brain (2.47 nmol $g^{-1}$). It is not clear why the DCN was not reported, to be consistent with the imaging regions of interest; it may be that dissecting this structure is difficult in the small rat brain. The same group reported additional studies repeating the aforementioned GBCA and adding comparison with two additional linear GBCAs (gadobenate dimeglumine and gadopentetate dimeglumine) and a saline control [63]. The same injection frequency was followed and results were consistent with their earlier study—the linear chelate groups demonstrated hyperintensity in the DCN and 4–14 times higher gadolinium levels in the cerebellum, while the macrocyclic compound had no effect. Modified injection protocols with twice a week or once a week injections for five weeks were also performed and yielded hyperintensity in the DCN after week six that persisted out to week 10 (last time point).

Similar studies were performed by administering four daily injections of gadodiamide (0.6 mmol Gd $kg^{-1}$) for five weeks on rats subjected to subtotal nephrectomy to create moderate renal impairment. Twofold higher gadolinium levels were observed in renally impaired rats in all brain structures studied, e.g. DCN (19.9 versus 12.3 ng $g^{-1}$), cerebellar parenchyma (10 versus 4.7 nmol $g^{-1}$) and brain stem (5.1 versus 2.6 nmol $g^{-1}$) [70]. Gadolinium was also elevated in bone. Hyperintensity was found in the DCN, as well as the choroid plexus in spite of low Gd found in the CSF (less than 0.05 µm $l^{-1}$).

A study in mice with renal failure, with a similar protocol of weekday daily injections for four weeks, examined retention of Gd-DTPA-BMA (5 mmol $kg^{-1}$), Gd-DOTA (5 mmol $kg^{-1}$) and $GdCl_3$ (0.2 mmol $kg^{-1}$) [73]. Tissues were analysed by ICP-MS after collection at 3 days or 45 days after the last injection. This is one of the longest time periods after injection that has been studied to date. Gadolinium levels were lower in all tissues for Gd-DOTA compared to Gd-DTPA. Levels of gadolinium in the brain decreased over time for both Gd-DOTA (1.4 µg $g^{-1}$ at day 3 to 0.2 µg $g^{-1}$ at day 45) and Gd-DTPA (5.04 µg $g^{-1}$ at day 3 to 2.6 µg $g^{-1}$ at day 45). Interestingly, no difference in long-term retention was observed between normal and renal failure mice. Mice with renal failure injected with $GdCl_3$ suffered from high attrition and could not be evaluated with statistical significance. In normal mice, a trend for decreasing retention was found for brain, spleen, skin and kidney, for both Gd-DOTA and Gd-DTPA, but liver values remained constant and bone values increased markedly for Gd-DTPA (in bone: 52.9 µg $g^{-1}$ at

day 3 to 203.3 µg $g^{-1}$ at day 45). In mice with renal failure, gadolinium retention decreased in all tissues by day 45 for Gd-DTPA. In these mice, for Gd-DOTA there was also a trend for decreasing Gd levels, but slight increases in liver and bone between days 3 and 45, which the authors [73] state is consistent with earlier studies that found elevated liver retention of contrast agent in renally impaired mice. Without the intermediate points, it is difficult to ascertain if this is a continuing trend of decrease or if some steady state is reached after injection but before 45 days.

Jost *et al*. [62] examined the same three linear chelates and two macrocycles (gadobutrol and gadoterate meglumine) using an injection frequency of 10 intravenous injections (5 days a week) over a period of two weeks at 2.5 mmol Gd $kg^{-1}$. The injected doses were quite a bit higher than in the studies above, and, though delivered over a shorter time period, they are still over double the total dose exposure (25 mmol, versus 12 mmol for Robert *et al.* [61,63]). Interestingly, their results differed somewhat from those above. Here, they found hyperintensity in the cerebellum (compared to the pons) for only two of the linear chelates, gadodiamide and gadobenate dimeglumine, and at 3 and 24 days after injection, with no significant changes in between these points. No statistically significant changes were found for gadopentetate or the macrocyclic GBCAs. Also, no elevated signal was found for the GP in any group. In addition, they performed fluid-attenuated MRI after injection of 1 mmol Gd $kg^{-1}$ GBCA to evaluate the CSF spaces. All five GBCAs tested were reported to demonstrate signal enhancement of the CSF, compared to no enhancement for the saline control, suggesting a potential route for GBCA to access the brain through leakage into the CSF. Note that gadobenate dimeglumine undergoes hepatic clearance. This work was followed up with another report by the same group using ICP-MS to examine the CSF, blood, cerebellum and pons after a single high dose (1.8 mmol $kg^{-1}$, three times the human dose) of GBCA; six different linear and macrocyclic compounds and one macromolecular agent were studied. CSF was obtained by stereotactic collection from the cisterna magna. At 4.5 h, 18.8–27.4 nmol $ml^{-1}$ of gadolinium was present in the CSF, but this decays to below blood gadolinium levels by 24 h (data summarized in figure 5). Lower amounts were observed for the macromolecular agent. There seems potential for a false positive with the 4 h CSF collection; at this time point, there is still circulating GBCA, as seen in the blood levels, and the act of insertion of the catheter capillary tube for sample collection could cause contamination with blood; given the high sensitivity of ICP-MS, even a small tainting with blood could skew the results. The MR images show hyperintensity in several CSF spaces. The volume and speed of injection were not provided, but as a bolus high dose, there is the potential for osmotic effects to disrupt the blood–CSF barrier or the BBB.

A more recent study exposed rats with up to 20 doses of gadodiamide (cumulative dose: 6 or 12 mmol $kg^{-1}$, low and high, respectively) over a five-week period (2–4 doses per week) [72]. Gadopentetate was included as a comparison point. Levels of gadolinium in the left hemisphere of the brain were measured at 1 and 20 weeks after dosing by ICP-MS, and the right hemisphere was used for histopathology. Gadolinium was found in the brain samples at one week post protocol and was significantly decreased by the 20-week time point (though still higher than saline). The high-dose group brains contained 2.49 nmol Gd $g^{-1}$ of tissue for gadodiamide compared to 1.4 nmol Gd $g^{-1}$ for gadopentetate, and 1.39 nmol Gd $g^{-1}$ for the low-dose group. No detectable gadolinium was found in the saline control brains. No evidence of toxic pathology was found in the histology. These results suggest that gadolinium is clearing, but much more slowly than in the two-compartment model previously described for gadodiamide, which experiences a rapid extracellular distribution on the order of minutes, followed by a slower elimination phase on the order of hours. In the studies by Smith *et al.* [72], there is an even longer elimination phase on the order of weeks. However, a clear trend towards clearance is observed. This may support that some element of pathology may contribute to the long-term gadolinium retention in the patient data reported so far, because the trend in normal animals is towards clearance to pre-contrast levels.

Another rat study of high dosing delivered 20 daily injections of one of four linear or two macrocyclic GBCAs at a dose of 2.5 mmol Gd $kg^{-1}$ [74]. Eight weeks after the last injection of

GBCA, brain and skin samples were collected for histological and ICP-MS analysis. These studies found 15-fold higher gadolinium levels in the brain for linear chelates than for macrocyclic; but, at the highest levels of retention, the amount of gadolinium in the brain was still less than 0.0002% of the injected dose $g^{-1}$ of tissue. On the other hand, fibrosis-like lesions, with infiltration of mononuclear cells, developed in the skin of some of the animals injected with gadodiamide, with corresponding higher levels of skin retention of gadolinium.

## (f) Mechanisms for how gadolinium accumulates in the brain

Is finding gadolinium in tissues really unexpected? The question remains as to whether gadolinium reaches the brain as a free ion or as a chelate. Gadolinium chelates do not typically cross the BBB. The blood–brain and blood–CSF barriers are generally impermeable to GBCAs, which have very low partition coefficients. When entering the brain, the chelate crosses both surfaces of the endothelial monolayer in the BBB, and, once across, must avoid clearance, such as through efflux transporters [75]. Although a rare occurrence, some reports have observed gadolinium distribution to the CSF; this is another potential route of access to the brain. For example, Hsu *et al.* present two case studies with diffuse CSF enhancement on MRI [76]. The patients had very different pathologies (one, a 5-year-old boy with a ventriculoperitoneal shunt (for hydrocephalus); the other, a 52-year-old man with glioblastoma multiforme), but both had potential leptomeningeal tumour spreading. In their discussion, the authors note that several reports have noted that there are a number of reports of disruption of the BBB upon intra-arterial injection of iodinated contrast media. At the time (2005), there were 16 literature reports of CSF enhancement for both charged (16 cases, gadopentetate dimeglumine) and charge-neutral (one case, gadodiamide) contrast agents. The difference in the number of cases may reflect the frequency of use of the agents as opposed to the particular effect on the CSF by charged versus charge-neutral agents. These authors make an interesting point, which seems particularly pertinent today, that the fenestrated capillaries of tumours could allow leakage of contrast agents into the CSF. Tumours near the choroid plexus and leptomeninges, principal sites of the interface for blood–CSF, could particularly allow access to CSF. It would be interesting to examine the tumour location in the cases of gadolinium deposition to date to see if there is any correlation with tumour location and contrast enhancement. The possibility of osmolarity-induced temporary BBB disruption with contrast administration also cannot be ruled out. Dissecting the means of injection as drip versus bolus for the known cases of deposition would also be interesting and a more detailed study for the presence of chelates in the CSF would be illuminating. A rat study by Rasschaert *et al.* [70], on the other hand, found hyperintensity of the choroid plexus 4 days after the last injection but the total Gd in CSF is less than 0.05 µmol Gd $l^{-1}$, suggesting that the enhancement is from the tissue not from CSF.

How could free gadolinium enter the brain? The primary mode of clearance for GBCA is renal filtration, depending upon the chelate, though some chelates are protein-bound and cleared through hepatocytes in the liver to be further cleared in faeces. The intravenous injection of GBCA skips first-pass clearance, giving the GBCA an opportunity to circulate once through the body before encountering the clearance systems of the kidney and liver. The kidney filters about 20% of the blood from the heart with each pump, and the 80% that does not go through the kidney circulates through the body, with potential for biological interactions and dilution in the blood, thus circulating back and having another chance to pass through the kidney. Kidney filtrates are excreted through the urine. However, like cutting pie segments continually into fifths, the level of GBCAs in blood exponentially decays and asymptotically approaches zero.

The lower formation constants ($K_f$) for linear chelates versus macrocyclic chelates make it logical to assume that the bonds between gadolinium and the more weakly chelating linear ligands can be broken more quickly and easily, releasing gadolinium ions. Still, from a chemist's perspective, chelates are very stable structures, which is why they were selected for their function in GBCAs. If one looks at the dissociation time instead of $K_f$, however, the picture might seem different. It has been reported that gadodiamide (Omniscan, GE HealthCare) has

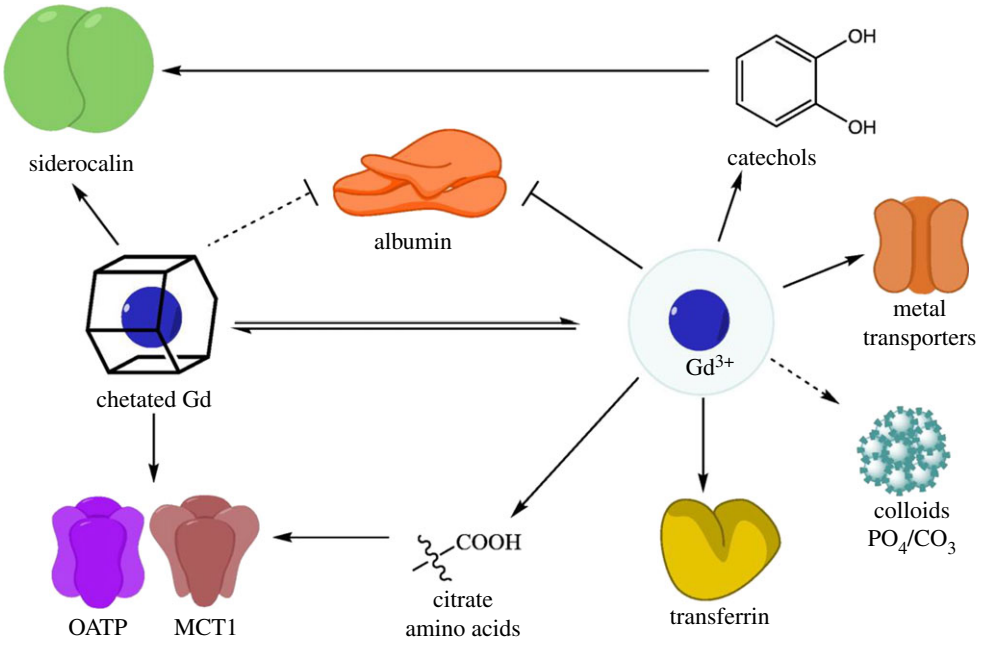


**Figure 6.** Proposed mechanisms for gadolinium or GBCA uptake into the brain. Each illustrated target is associated with processes that result in delivery of metals to the CNS, or has been proposed as an uptake mechanism. Binding targets of gadolinium or chelated gadolinium associated with uptake are indicated by an arrow, and processes that limit uptake (i.e. binding to albumin) are denoted by a bar. As all GBCAs do not bind albumin, and evidence exists supporting both increased and decreased uptake of colloids, those lines are dashed. $CO_3$, carbonate; Gd, gadolinium; MCT1, monocarboxylate transporter 1; OATP, organic anion-transporting polypeptide; $PO_4$, phosphate. Adapted from [78]. (Online version in colour.)

a 30 s dissociation time, compared to 3 h for the macrocyclic gadoteridol (ProHance, Bracco Diagnostics) [66]. Weigh this against the 1.5 h half-life of gadolinium chelates in patients with normal renal function and the 6 h half-life in a patient with chronic kidney disease ($34 \pm 22$ h has been reported as a half-life for gadodiamide for patients with severe renal insufficiency [77]), and the possibility for release of gadolinium from the chelate seems more likely. It is estimated that approximately 90% of the injected dose of GBCA, for most approved GBCAs, in patients with normal renal function, is excreted in 24 h. By contrast, it would take 5 days for 76% of gadobutrol to be recovered in patients with severe renal impairment (creatine less than 10 ml $min^{-1}$) [1]. One can see that it is possible for a non-zero fraction of GBCA to circulate over periods of time much longer than the dissociation constant, particularly for renally compromised patients. This prolonged circulation increases the probability for release of gadolinium over time.

It has been proposed that free gadolinium could enter the brain through any number of processes known to transport metals into the brain, as illustrated in figure 6. Given the size and the coordination environment for gadolinium, and the specificity of metal-binding proteins in these pathways, most of these processes seem unlikely. Gadolinium is known as a potent calcium channel blocker but does not itself seem to be able to travel through the channels as a free ion [79,80]. However, colloidal deposition is feasible and consistent with the early SEM/EDS results on phosphate deposits.

However, because most of the reports of brain accumulation to date have been for patients with brain tumour or other neurologic complications, one cannot rule out that BBB permeability allows intact chelate into the brain, which then is vulnerable to transmetallation. This view is consistent with the hypothesis that the hyperintense dentate nucleus has high levels of endogenous metals such as zinc and iron (abundant at the periphery) and copper (localized around the nucleus) [81];

these endogenous ions are capable of displacing gadolinium from the gadolinium complex, zinc particularly. However, they are found inside the cell, so there remains the question of how chelates could enter the cell. Furthermore, zinc, calcium and iron are high in other regions of the brain that do not experience hyperintensity. For example, the substantia nigra is high in iron, and is not implicated in hyperintensity until very high numbers of repeated injections are reached. Although high iron may contribute to transmetallation, the high iron $T_2$* background may counterbalance smaller intensity changes, and ICP-MS or other methods should be performed to confirm lack of accumulation.

## 4. Conclusion

The human and animal studies to date generally confirm a long-term retention of gadolinium in the brain that was perhaps unexpected; however, most of these patients had underlying disease that could affect the BBB. In addition, studies primarily focused on patients with and without renal insufficiency who had received multiple injections of GBCA. Animal studies largely echo the observations from human tissues, and again deposits are observed after multiple injections or high-dose bolus. The amounts of gadolinium retained were generally extremely low, and the lanthanide is present either in such low amounts or in such a form as to not cause obvious adverse biological effects. How deposits form can be plausibly explained by the low solubility of free gadolinium at neutral pH.

Other biological factors unrelated to frequency or dose of delivery can affect the serum stability of GBCAs. For example, past literature noted a decrease in stability for linear GBCAs, but not for macrocyclic GBCAs, in serum in the presence of elevated phosphate levels [44]. This is particularly interesting, as renal failure strongly disrupts calcium and phosphorus balance, and results in phosphorus retention (hyperphosphataemia) as well as vascular calcification [82]. This imbalance results in calcium precipitation as $CaHPO_4$. We could, thus, envisage that, in patients with renal insufficiency, the phosphate imbalance contributes to GBCA instability. Can phosphate explain cases with normal renal function? A recent study identified high inorganic phosphate in highly metastatic tumours in a mouse breast cancer model (double compared to non-metastatic) as a marker of tumour progression (both types of tumours were high in phosphorus levels compared to normal mammary gland) [83]. One could envisage leaky tumour vasculature allowing the penetration of chelates into the tumour, where high phosphate levels exacerbate instability and also provide counter-ions for the eventual formation of precipitates. Phosphorus could be acting as both the devil (destabilizing chelate) and the saviour (precipitating free gadolinium ions) in this process. It is not known if high plasma phosphate translates to high phosphate in the CSF; however, in hyperphosphataemia there is elevated ammonia in the brain; this could result in high –OH levels, which can destabilize the chelation of GBCA in the CSF.

There is likely to be a combination of different pathways that could lead to accumulation of gadolinium in the brain, which will vary with each patient depending upon their disease pathology and the frequency/mode/type/dose of GBCA administered. BBB compromise due to disease, high phosphorus from renal insufficiency, osmotic effect of GBCA injection, leaky CSF in disease over time and with multiple injections, each of these pathways could contribute to the retention of gadolinium in the brain. We illustrate these putative pathways in figure 7.

Both the occurrence of NSF and gadolinium accumulation in the brain underscore the need for extremely stable contrast agents, careful handling of patients with renal insufficiency and also careful consideration of the need for repeated contrast-enhanced procedures. Different chemical strategies have been exploited to improve the stability of contrast agents *in vivo* while not sacrificing their contrast-enhancing efficacy. For example, changing the basicity, rigidity and cavity size of the macrocyclic ligand has been demonstrated to influence the thermodynamic stability of gadolinium-based complexes [84]. In designing GBCAs, the stability of the chelate against dissociation and transmetallation *in vivo* is a better indicator for *in vivo* safety when compared with thermodynamic stability.

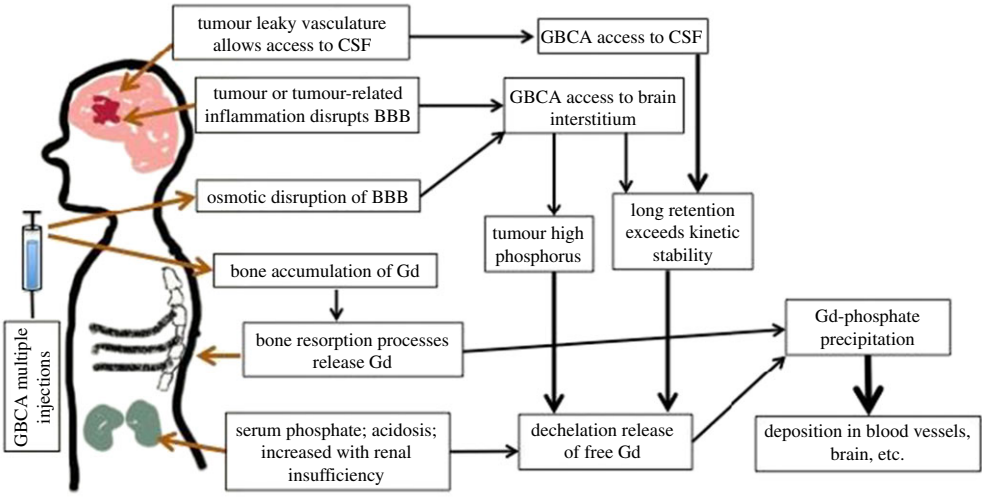


**Figure 7.** Possible physiological routes for GBCA or free Gd accumulation and dechelation, in the body. Tumour-related processes can lead to leakage of GBCA into the CSF or interstitium; over long periods of time, GBCA can release Gd. High bolus injections of charged GBCA can open the BBB to allow GBCA access to the brain. The high serum phosphate in renal insufficiency can destabilize GBCA to release Gd. It is known that Gd can accumulate in bone; in aging, menopause and other processes of bone resorption and remodelling, Gd can be released. Free Gd released from any of these routes is unstable at physiological pH and precipitates as gadolinium hydroxides or phosphates, resulting in the formation of deposits in capillary beds. (Online version in colour.)

In addition to ligand design, designing agents using safer paramagnetic metal ions such as manganese is an alternative approach. While high concentration of free manganese ions can impart neurotoxicity ($LD_{50}$ of aqueous manganese $= 0.3\,\mathrm{mmol\,kg^{-1}}$ in mice, IV), chelated manganese-based contrast agents are generally deemed safer. The only clinically approved manganese-based contrast agent, manganese(II) dipyridoxaldiphosphate (Mn-DPDP), has a significantly higher safety factor [85] ($LD_{50}$/effective dose of 540) than the gadolinium-based Gd-DTPA (Magnevist, $LD_{50}$/effective dose of 60–100), indicating a promising alternative for GBCAs. Most recent approaches in the development of manganese-based contrast agents are presented in a review by Pan *et al.* [86] and we refer the interested reader to this resource.

Magnetic iron oxide nanoparticles are touted for their superior safety profile over GBCAs. Unlike GBCAs, these nanoparticles have good biocompatibility as they can be cleared from the blood to the liver via the reticuloendothelial system (RES) and can be metabolized to join endogenous iron stores [87,88]. However, iron-based contrast agents have not fared well commercially. While several superparamagnetic iron oxide nanoparticle (SPIO) preparations have been clinically tested, some did not receive regulatory approval and some were not developed further after failing to demonstrate sufficient clinical efficacy. For example, in 2007 Guerbet withdrew its application for a marketing authorization for Sinerem because 'the main study used to evaluate the benefit–risk profile of the medicine had failed to statistically demonstrate the efficacy of Sinerem'. The limited clinical predictive quality of SPIO in a number of applications tested, including lymph node and liver imaging, has resulted in attrition in the availability of clinically approved agents; Feridex is no longer commercially available in the USA, and Resovist, approved for Europe, is only available in a few countries. In the light of these difficulties, other agents have been 'repurposed', such as Ferumoxytol, which is approved for treatment of iron deficiency in adult chronic kidney patients [89]. Other disadvantages for SPIO are related to its nature as a $T_2$ contrast agent, and include difficulty in differentiating signals from the negative contrast agents and the background, occurrence of susceptibility artefacts, slow clearance for large nanoparticle sizes (greater than 60 nm) and longer processing time for

$T_2$-weighted MR imaging relative to $T_1$-weighted imaging [88]. Introduction of gadolinium-based agents onto the surface of iron-oxide-based nanoparticles is one approach to address the inherent disadvantage of using either $T_1$ or $T_2$ agents [17,90,91]. For example, a nanoparticle ($MnFe_2O_4$@$SiO_2$@$Gd_2O_3$) [90] showed ON response for both $T_1$ and $T_2$ modes, while Gd-DTPA and Feridex showed OFF response in $T_1$ and $T_2$ modes, respectively. This property gives MR imaging a self-confirming ability and is expected to improve accuracy in MR image analysis. While these dual-imaging nanoprobes show promise for diagnostic applications, there is still much that needs to be investigated, including the safety profile of these nanoprobes. Recently, Zeng *et al.* [92] reported ultra-small (4–5 nm) iron oxide nanoparticles $MFe_2O_4$ (M = Fe, Zn, Ni) with good water solubility and low cytotoxicity and potential as $T_1$ agents. The longitudinal relaxivity $r_1$ of these nanoparticles was in the range of 5.991–7.928 $mM^{-1}\,s^{-1}$ (0.5 T), which is comparable to clinically approved GBCAs. The advantages of nanoparticles include reduced RES uptake compared to micrometre-sized particles, longer circulation time than renally excreted compounds, and a circulation time in the blood that can be tuned by controlling nanoparticle size and coating functionality. Further, systematic probe design through surface modification of iron oxide nanoparticles enables the use of these nanoparticles for a variety of applications such as targeted and multimodal positron emission tomography/MR imaging [93,94]. Combined with $T_1$ detection and low cytotoxicity, the attractiveness of iron oxides may come to shine again in the wake of gadolinium's deposition issues.

At present, the retention of gadolinium observed in brains seems more a curiosity than a health concern. The low levels of retained gadolinium suggest that, even if this were in the form of free gadolinium, it is well below toxic levels; however, long-term sequestration of any toxic metal, even in an inert state, in a sensitive structure such as the brain, is concerning. The fear is that there could be a point in the lifespan where pathological or other processes could release gadolinium and pose a risk for the local concentration of gadolinium to reach pathological levels or for the deposits themselves to do harm (e.g. vascular emboli). Further health effect and mechanistic studies are warranted that will aid in the design of treatment protocols as well as define appropriate agents for use in patients with renal insufficiency. With time, we hope that research will shed light on whether we have anything to fear.

> Fears are educated into us, and can, if we wish, be educated out.
>
> Karl Augustus Menninger

Data accessibility. This article has no additional data.

Authors' contributions. A.Y.L. conceived of the article. J.G. and A.Y.L. drafted and revised the article. S.Z.L. contributed table 2 and to article revision. All three authors approved the final version of the article.

Competing interests. We declare that we have no competing interests.

Funding. J.G., S.Z.L. and A.Y.L thank the KECK Foundation for financial support.

## References

1. Aime S, Caravan P. 2009 Biodistribution of gadolinium-based contrast agents, including gadolinium deposition. *J. Magn. Reson. Imaging* **30**, 1259–1267. (doi:10.1002/jmri.21969)
2. Lowes R. 2013 *FDA approves new gadolinium-based MRI agent*. See http://www.medscape.com/viewarticle/781144.
3. European Medicines Agency. 2010 *Assessment report for gadolinium-containing contrast agents*. See http://www.ema.europa.eu/docs/en_GB/document_library/Referrals_document/gadolinium_31/WC500099538.pdf.
4. McDonald RJ, McDonald JS, Kallmes DF, Jentoft ME, Murray DL, Thielen KR, Williamson EE, Eckel LJ. 2015 Intracranial gadolinium deposition after contrast-enhanced MR imaging. *Radiology* **275**, 772–782. (doi:10.1148/radiol.15150025)
5. Ramalho J, Castillo M, AlObaidy M, Nunes RH, Ramalho M, Dale BM, Semelka RC. 2015 High signal intensity in globus pallidus and dentate nucleus on unenhanced $T_1$-weighted MR images: evaluation of two linear gadolinium-based contrast agents. *Radiology* **276**, 836–844. (doi:10.1148/radiol.2015150872)

6. Ichikawa S, Motosugi U, Omiya Y, Onishi H. 2017 Contrast agent–induced high signal intensity in dentate nucleus on unenhanced $T_1$-weighted images: comparison of gadodiamide and gadoxetic acid. *Invest. Radiol.* **52**, 389–395. (doi:10.1097/RLI.0000000000000360)
7. McDonald JS, McDonald RJ, Jentoft ME, Paolini MA, Murray DL, Kallmes DF, Eckel L. 2017 Intracranial gadolinium deposition following gadodiamide-enhanced magnetic resonance imaging in pediatric patients: a case-control study. *JAMA Pediatr.* **171**, 705–707. (doi:10.1001/jamapediatrics.2017.0264)
8. Quattrocchi CC, Mallio CA, Errante Y, Cirimele V, Carideo L, Ax A, Zobel BB. 2015 Gadodiamide and dentate nucleus $T_1$ hyperintensity in patients with meningioma evaluated by multiple follow-up contrast-enhanced magnetic resonance examinations with no systemic interval therapy. *Invest. Radiol.* **50**, 470–472. (doi:10.1097/RLI.0000000000000154)
9. Kanda T, Ishii K, Kawaguchi H, Kitajima K, Takenaka D. 2014 High signal intensity in the dentate nucleus and globus pallidus on unenhanced $T_1$-weighted MR images: relationship with increasing cumulative dose of a gadolinium-based contrast material. *Radiology* **270**, 834–841. (doi:10.1148/radiol.13131669)
10. Forslin Y, Shams S, Hashim F, Aspelin P, Bergendal G, Martola J, Fredrikson S, Kristoffersen-Wiberg M, Granberg T. 2017 Retention of gadolinium-based contrast agents in multiple sclerosis: retrospective analysis of an 18-year longitudinal study. *Am. J. Neuroradiol.* **38**, 1311–1316. (doi:10.3174/ajnr.A5211)
11. Errante Y, Cirimele V, Mallio CA, Di Lazzaro V, Zobel BB, Quattrocchi CC. 2014 Progressive increase of $T_1$ signal intensity of the dentate nucleus on unenhanced magnetic resonance images is associated with cumulative doses of intravenously administered gadodiamide in patients with normal renal function, suggesting dechelation. *Invest. Radiol.* **49**, 685–690. (doi:10.1097/RLI.0000000000000072)
12. Tanaka M, Nakahara K, Kinoshita M. 2016 Increased signal intensity in the dentate nucleus of patients with multiple sclerosis in comparison with neuromyelitis optica spectrum disorder after multiple doses of gadolinium contrast. *Eur. Neurol.* **75**, 195–198. (doi:10.1159/000445431)
13. Kanda T, Fukusato T, Matsuda M, Toyoda K, Oba H, Ji K, Haruyama T, Kitajima K, Furui S. 2015 Gadolinium-based contrast agent accumulates in the brain even in subjects without severe renal dysfunction: evaluation of autopsy brain specimens with inductively coupled plasma mass spectroscopy. *Radiology* **276**, 228–232. (doi:10.1148/radiol.2015142690)
14. Zhang Y, Cao Y, Shih GL, Hecht EM, Prince MR. 2016 Extent of signal hyperintensity on unenhanced $T_1$-weighted brain MR images after more than 35 administrations of linear gadolinium-based contrast agents. *Radiology* **2016**, 152864. (doi:10.1148/radiol.2016152864)
15. Ramalho J, Semelka RC, AlObaidy M, Ramalho M, Nunes RH, Castillo M. 2016 Signal intensity change on unenhanced $T_1$-weighted images in dentate nucleus following gadobenate dimeglumine in patients with and without previous multiple administrations of gadodiamide. *Eur. Radiol.* **26**, 4080–4088. (doi:10.1007/s00330-016-4269-7)
16. Xia D, Davis RL, Crawford JA, Abraham JL. 2010 Gadolinium released from MR contrast agents is deposited in brain tumors: *in situ* demonstration using scanning electron microscopy with energy dispersive X-ray spectroscopy. *Acta Radiol.* **51**, 1126–1136. (doi:10.3109/02841851.2010.515614)
17. Keasberry NA, Bañobre-López M, Wood C, Stasiuk GJ, Gallo J, Long NJ. 2015 Tuning the relaxation rates of dual-mode $T_1/T_2$ nanoparticle contrast agents: a study into the ideal system. *Nanoscale* **7**, 16 119–16 128. (doi:10.1039/C5NR04400F)
18. Radbruch A *et al.* 2015 Gadolinium retention in the dentate nucleus and globus pallidus is dependent on the class of contrast agent. *Radiology* **275**, 783–791. (doi:10.1148/radiol.2015150337)
19. Cao Y, Huang DQ, Shih G, Prince MR. 2016 Signal change in the dentate nucleus on $T_1$-weighted MR images after multiple administrations of gadopentetate dimeglumine versus gadobutrol. *Am. J. Roentgenol.* **206**, 414–419. (doi:10.2214/AJR.15.15327)
20. Flood TF, Stence NV, Maloney JA, Mirsky DM. 2017 Pediatric brain: repeated exposure to linear gadolinium-based contrast material is associated with increased signal intensity at unenhanced $T_1$-weighted MR imaging. *Radiology* **282**, 222–228. (doi:10.1148/radiol.2016160356)

21. Miller JH, Hu HH, Pokorney A, Cornejo P, Towbin R. 2015 MRI brain signal intensity changes of a child during the course of 35 gadolinium contrast examinations. *Pediatrics* **136**, e1637–e1640. (doi:10.1542/peds.2015-2222)
22. Adin M, Kleinberg L, Vaidya D, Zan E, Mirbagheri S, Yousem D. 2015 Hyperintense dentate nuclei on $T_1$-weighted MRI: relation to repeat gadolinium administration. *Am. J. Neuroradiol.* **36**, 1859–1865. (doi:10.3174/ajnr.A4378)
23. Khant ZA, Hirai T, Kadota Y, Masuda R, Yano T, Azuma M, Suzuki Y, Tashiro K. 2017 $T_1$ shortening in the cerebral cortex after multiple administrations of gadolinium-based contrast agents. *Magn. Reson. Med. Sci.* **16**, 84–86. (doi:10.2463/mrms.mp.2016-0054)
24. Weberling LD, Kieslich PJ, Kickingereder P, Wick W, Bendszus M, Schlemmer H-P, Radbruch A. 2015 Increased signal intensity in the dentate nucleus on unenhanced $T_1$-weighted images after gadobenate dimeglumine administration. *Invest. Radiol.* **50**, 743–748. (doi:10.1097/RLI.0000000000000206)
25. Murata N, Gonzalez-Cuyar LF, Murata K, Fligner C, Dills R, Hippe D, Maravilla KR. 2016 Macrocyclic and other non-group 1 gadolinium contrast agents deposit low levels of gadolinium in brain and bone tissue: preliminary results from 9 patients with normal renal function. *Invest. Radiol.* **51**, 447–453. (doi:10.1097/RLI.0000000000000252)
26. Kromrey M-L, Liedtke KR, Ittermann T, Langner S, Kirsch M, Weitschies W, Kühn J-P. 2017 Intravenous injection of gadobutrol in an epidemiological study group did not lead to a difference in relative signal intensities of certain brain structures after 5 years. *Eur. Radiol.* **27**, 772–777. (doi:10.1007/s00330-016-4418-z)
27. Stojanov DA, Aracki-Trenkic A, Vojinovic S, Benedeto-Stojanov D, Ljubisavljevic S. 2016 Increasing signal intensity within the dentate nucleus and globus pallidus on unenhanced $T_1$ W magnetic resonance images in patients with relapsing-remitting multiple sclerosis: correlation with cumulative dose of a macrocyclic gadolinium-based contrast agent, gadobutrol. *Eur. Radiol.* **26**, 807–815. (doi:10.1007/s00330-015-3879-9)
28. Agris J, Pietsch H, Balzer T. 2016 What evidence is there that gadobutrol causes increasing signal intensity within the dentate nucleus and globus pallidus on unenhanced $T_1$ W MRI in patients with RRMS? *Eur. Radiol.* **26**, 816–817. (doi:10.1007/s00330-015-4019-2)
29. Kanda T, Oba H, Toyoda K, Furui S. 2016 Macrocyclic gadolinium-based contrast agents do not cause hyperintensity in the dentate nucleus. *Am. J. Neuroradiol.* **37**, E41. (doi:10.3174/ajnr.A4710)
30. Radbruch A *et al.* 2017 Pediatric brain: no increased signal intensity in the dentate nucleus on unenhanced $T_1$-weighted MR images after consecutive exposure to a macrocyclic gadolinium-based contrast agent. *Radiology* **283**, 828–836. (doi:10.1148/radiol.2017162980)
31. Eisele P, Alonso A, Szabo K, Ebert A, Ong M, Schoenberg SO, Gass A. 2016 Lack of increased signal intensity in the dentate nucleus after repeated administration of a macrocyclic contrast agent in multiple sclerosis: an observational study. *Medicine* **95**, e4624. (doi:10.1097/MD.0000000000004624)
32. Eisele P, Szabo K, Alonso A, Ong M, Platten M, Schoenberg SO, Gass A. 2017 Lack of $T_1$ hyperintensity in the dentate nucleus after 15 administrations of a macrocyclic contrast agent in multiple sclerosis. *J. Neurol. Neurosurg. Psychiatry*. (doi:10.1136/jnnp-2017-316102)
33. Espagnet MCR, Bernardi B, Pasquini L, Talamanca L, Tomà P, Napolitano A. 2017 Erratum to: Signal intensity at unenhanced $T_1$-weighted magnetic resonance in the globus pallidus and dentate nucleus after serial administrations of a macrocyclic gadolinium-based contrast agent in children. *Pediatr. Radiol.* **47**, 1366. (doi:10.1007/s00247-017-3950-6)
34. Thomsen HS, Marckmann P, Logager VB. 2007 Nephrogenic systemic fibrosis (NSF): a late adverse reaction to some of the gadolinium based contrast agents. *Cancer Imaging* **7**, 130. (doi:10.1102/1470-7330.2007.0019)
35. Caille JM, Lemanceau B, Bonnemain B. 1983 Gadolinium as a contrast agent for NMR. *Am. J. Neuroradiol.* **4**, 1041–1042. See https://www.ncbi.nlm.nih.gov/pubmed/6414266.
36. Grobner T. 2006 Gadolinium–a specific trigger for the development of nephrogenic fibrosing dermopathy and nephrogenic systemic fibrosis? *Nephrol. Dial. Transplant.* **21**, 1104–1108. (doi:10.1093/ndt/gfk062)
37. Bleavins K *et al.* 2012 Stimulation of fibroblast proliferation by insoluble gadolinium salts. *Biol. Trace Elem. Res.* **145**, 257–267. (doi:10.1007/s12011-011-9176-9)

38. Ramalho J, Semelka RC, Ramalho M, Nunes R, AlObaidy M, Castillo M. 2016 Gadolinium-based contrast agent accumulation and toxicity: an update. *Am. J. Neuroradiol.* **37**, 1192–1198. (doi:10.3174/ajnr.A4615)
39. Sherry AD, Caravan P, Lenkinski RE. 2009 Primer on gadolinium chemistry. *J. Magn. Reson. Imaging* **30**, 1240–1248. (doi:10.1002/jmri.21966)
40. Gamage NDH, Mei Y, Garcia J, Allen MJ. 2010 Oxidatively stable, aqueous europium(II) complexes through steric and electronic manipulation of cryptand coordination chemistry. *Angew. Chem. Int. Edn.* **49**, 8923–8925. (doi:10.1002/anie.201002789)
41. Garcia J, Kuda-Wedagedara AN, Allen MJ. 2012 Physical properties of $Eu^{2+}$-containing cryptates as contrast agents for ultrahigh-field magnetic resonance imaging. *Eur. J. Inorg. Chem.* **2012**, 2135–2140. (doi:10.1002/ejic.201101166)
42. Idée J-M, Fretellier N, Robic C, Corot C. 2014 The role of gadolinium chelates in the mechanism of nephrogenic systemic fibrosis: a critical update. *Crit. Rev. Toxicol.* **44**, 895–913. (doi:10.3109/10408444.2014.955568)
43. Heverhagen J, Krombach G, Gizewski E. 2014 Application of extracellular gadolinium-based MRI contrast agents and the risk of nephrogenic systemic fibrosis. *Röfo* (*Fortschr. Röntgenstr.*) **186** (7), 661–669. (doi:10.1055/s-0033-1356403)
44. Frenzel T, Lengsfeld P, Schirmer H, Hütter J, Weinmann H-J. 2008 Stability of gadolinium-based magnetic resonance imaging contrast agents in human serum at 37°C. *Invest. Radiol.* **43**, 817–828. (doi:10.1097/RLI.0b013e3181852171)
45. Sieber MA *et al.* 2008 Preclinical investigation to compare different gadolinium-based contrast agents regarding their propensity to release gadolinium *in vivo* and to trigger nephrogenic systemic fibrosis-like lesions. *Eur. Radiol.* **18**, 2164–2173. (doi:10.1007/s00330-008-0977-y)
46. Sieber MA, Pietsch H, Walter J, Haider W, Frenzel T, Weinmann H-J. 2008 A preclinical study to investigate the development of nephrogenic systemic fibrosis: a possible role for gadolinium-based contrast media. *Invest. Radiol.* **43**, 65–75. (doi:10.1097/RLI.0b013e31815e6277)
47. Abraham J, Thakral C, Skov L, Rossen K, Marckmann P. 2008 Dermal inorganic gadolinium concentrations: evidence for *in vivo* transmetallation and long-term persistence in nephrogenic systemic fibrosis. *Br. J. Dermatol.* **158**, 273–280. (doi:10.1111/j.1365-2133.2007.08335.x)
48. George SJ, Webb SM, Abraham JL, Cramer SP. 2010 Synchrotron X-ray analyses demonstrate phosphate-bound gadolinium in skin in nephrogenic systemic fibrosis. *Br. J. Dermatol.* **163**, 1077–1081. (doi:10.1111/j.1365-2133.2010.09918.x)
49. Rowe PS, Zelenchuk LV, Laurence JS, Lee P, Brooks WM, McCarthy ET. 2015 Do ASARM peptides play a role in nephrogenic systemic fibrosis? *Am. J. Physiol. Renal Physiol.* **309**, F764–F769. (doi:10.1152/ajprenal.00201.2015)
50. Marckmann P *et al.* 2006 Nephrogenic systemic fibrosis: suspected causative role of gadodiamide used for contrast-enhanced magnetic resonance imaging. *J. Am. Soc. Nephrol.* **17**, 2359–2362. (doi:10.1681/ASN.2006060601)
51. Cowper SE, Bucala R, Leboit PE. 2006 Nephrogenic fibrosing dermopathy/nephrogenic systemic fibrosis—setting the record straight. *Semin. Arthritis Rheum.* **35** (4), 208–210. (doi:10.1016/j.semarthrit.2005.09.005)
52. Darrah TH, Prutsman-Pfeiffer JJ, Poreda RJ, Campbell ME, Hauschka PV, Hannigan RE. 2009 Incorporation of excess gadolinium into human bone from medical contrast agents. *Metallomics* **1**, 479–488. (doi:10.1039/b905145g)
53. Gibby WA, Gibby KA, Gibby WA. 2004 Comparison of Gd DTPA-BMA (Omniscan) versus Gd HP-DO3A (ProHance) retention in human bone tissue by inductively coupled plasma atomic emission spectroscopy. *Invest. Radiol.* **39**, 138–142. (doi:10.1097/01.rli.0000112789.57341.01)
54. Rogosnitzky M, Branch S. 2016 Gadolinium-based contrast agent toxicity: a review of known and proposed mechanisms. *Biometals* **29**, 365–376. (doi:10.1007/s10534-016-9931-7)
55. White GW, Gibby WA, Tweedle MF. 2006 Comparison of Gd(DTPA-BMA) (Omniscan) versus Gd(HP-DO3A) (ProHance) relative to gadolinium retention in human bone tissue by inductively coupled plasma mass spectroscopy. *Invest. Radiol.* **41**, 272–278. (doi:10.1097/01.rli.0000186569.32408.95)

56. Montagne A, Toga AW, Zlokovic BV. 2016 Blood–brain barrier permeability and gadolinium: benefits and potential pitfalls in research. *JAMA Neurol.* **73**, 13–14. (doi:10.1001/jamaneurol.2015.2960)
57. Spencer A, Wilson S, Harpur E. 1998 Gadolinium chloride toxicity in the mouse. *Hum. Exp. Toxicol.* **17**, 633–637. (doi:10.1177/096032719801701108)
58. Spencer AJ, Wilson SA, Batchelor J, Reid A, Rees J, Harpur E. 1997 Gadolinium chloride toxicity in the rat. *Toxicol. Pathol.* **25**, 245–255. (doi:10.1177/019262339702500301)
59. Alves FC *et al.* 2003 Silencing of phosphonate-gadolinium magnetic resonance imaging contrast by hydroxyapatite binding. *Invest. Radiol.* **38**, 750–760. (doi:10.1097/01.rli.0000084891.15996.0f)
60. Sanyal S, Marckmann P, Scherer S, Abraham JL. 2011 Multiorgan gadolinium (Gd) deposition and fibrosis in a patient with nephrogenic systemic fibrosis—an autopsy-based review. *Nephrol. Dial. Transplant.* **26**, 3616–3626. (doi:10.1093/ndt/gfr085)
61. Robert P, Lehericy S, Grand S, Violas X, Fretellier N, Idée J-M, Ballet S, Corot C. 2015 $T_1$-weighted hypersignal in the deep cerebellar nuclei after repeated administrations of gadolinium-based contrast agents in healthy rats: difference between linear and macrocyclic agents. *Invest. Radiol.* **50**, 473–480. (doi:10.1097/RLI.0000000000000181)
62. Jost G, Lenhard DC, Sieber MA, Lohrke J, Frenzel T, Pietsch H. 2016 Signal increase on unenhanced $T_1$-weighted images in the rat brain after repeated, extended doses of gadolinium-based contrast agents: comparison of linear and macrocyclic agents. *Invest. Radiol.* **51**, 83. (doi:10.1097/RLI.0000000000000242)
63. Robert P, Violas X, Grand S, Lehericy S, Idée J-M, Ballet S, Corot C. 2016 Linear gadolinium-based contrast agents are associated with brain gadolinium retention in healthy rats. *Invest. Radiol.* **51**, 73. (doi:10.1097/RLI.0000000000000241)
64. Popescu BFG, Robinson CA, Rajput A, Rajput AH, Harder SL, Nichol H. 2009 Iron, copper, and zinc distribution of the cerebellum. *Cerebellum* **8**, 74–79. (doi:10.1007/s12311-008-0091-3)
65. Birka M, Wentker KS, Lusmöller E, Arheilger B, Wehe CA, Sperling M, Stadler R, Karst U. 2015 Diagnosis of nephrogenic systemic fibrosis by means of elemental bioimaging and speciation analysis. *Anal. Chem.* **87**, 3321–3328. (doi:10.1021/ac504488k)
66. Penfield JG, Reilly RF. 2007 What nephrologists need to know about gadolinium. *Nat. Clin. Pract. Nephrol.* **3**, 654–668. (doi:10.1038/ncpneph0660)
67. Radbruch A. 2016 Are some agents less likely to deposit gadolinium in the brain? *Magn. Reson. Imaging* **34**, 1351–1354. (doi:10.1016/j.mri.2016.09.001)
68. Ramalho J, Ramalho M, AlObaidy M, Semelka RC. 2016 Technical aspects of MRI signal change quantification after gadolinium-based contrast agents' administration. *Magn. Reson. Imaging* **34**, 1355–1358. (doi:10.1016/j.mri.2016.09.004)
69. Fretellier N *et al.* 2015 Distribution profile of gadolinium in gadolinium chelate-treated renally-impaired rats: role of pharmaceutical formulation. *Eur. J. Pharm. Sci.* **72**, 46–56. (doi:10.1016/j.ejps.2015.02.016)
70. Rasschaert M, Idée JM, Robert P, Fretellier N, Vives V, Violas X, Ballet S, Corot C. 2017 Moderate renal failure accentuates $T_1$ signal enhancement in the deep cerebellar nuclei of gadodiamide-treated rats. *Invest. Radiol.* **52**, 255–264. (doi:10.1097/RLI.0000000000000339)
71. Jost G, Frenzel T, Lohrke J, Lenhard DC, Naganawa S, Pietsch H. 2017 Penetration and distribution of gadolinium-based contrast agents into the cerebrospinal fluid in healthy rats: a potential pathway of entry into the brain tissue. *Eur. Radiol.* **27**, 2877–2885. (doi:10.1007/s00330-016-4654-2)
72. Smith AP, Marino M, Roberts J, Crowder JM, Castle J, Lowery L, Morton C, Hibberd MG, Evans PM. 2016 Clearance of gadolinium from the brain with no pathologic effect after repeated administration of gadodiamide in healthy rats: an analytical and histologic study. *Radiology* **282**, 743–751. (doi:10.1148/radiol.2016160905)
73. Kartamihardja AAP, Nakajima T, Kameo S, Koyama H, Tsushima Y. 2016 Impact of impaired renal function on gadolinium retention after administration of gadolinium-based contrast agents in a mouse model. *Invest. Radiol.* **51**, 655–660. (doi:10.1097/RLI.0000000000000295)
74. Lohrke J *et al.* 2017 Histology and gadolinium distribution in the rodent brain after the administration of cumulative high doses of linear and macrocyclic gadolinium-based contrast agents. *Invest. Radiol.* **52**, 324–333. (doi:10.1097/RLI.0000000000000344)

75. Hammarlund-Udenaes M, Fridén M, Syvänen S, Gupta A. 2008 On the rate and extent of drug delivery to the brain. *Pharm. Res.* **25**, 1737–1750. (doi:10.1007/s11095-007-9502-2)
76. Hsu HL, Chen CJ. 2005 Extensive cerebrospinal fluid enhancement following gadolinium chelate administration: possible pathogenesis. *Acta Radiol.* **46**, 523–527. (doi:10.1080/02841850510021472)
77. Joffe P, Thomsen HS, Meusel M. 1998 Pharmacokinetics of gadodiamide injection in patients with severe renal insufficiency and patients undergoing hemodialysis or continuous ambulatory peritoneal dialysis. *Acad. Radiol.* **5**, 491–502. (doi:10.1016/S1076-6332(98)80191-8)
78. Prybylski JP, Maxwell E, Sanchez CC, Jay M. 2016 Gadolinium deposition in the brain: lessons learned from other metals known to cross the blood–brain barrier. *Magn. Reson. Imaging* **34**, 1366–1372. (doi:10.1016/j.mri.2016.08.018)
79. Cheng Y, Liu M, Li R, Wang C, Bai C, Wang K. 1999 Gadolinium induces domain and pore formation of human erythrocyte membrane: an atomic force microscopic study. *Biochim. Biophys. Acta* **1421**, 249–260. (doi:10.1016/S0005-2736(99)00125-X)
80. Lacampagne A, Gannier F, Argibay J, Garnier D, Le Guennec J-Y. 1994 The stretch-activated ion channel blocker gadolinium also blocks L-type calcium channels in isolated ventricular myocytes of the guinea-pig. *Biochim. Biophys. Acta* **1191**, 205–208. (doi:10.1016/0005-2736(94)90250-X)
81. Runge VM. 2016 Safety of the gadolinium-based contrast agents for magnetic resonance imaging, focusing in part on their accumulation in the brain and especially the dentate nucleus. *Invest. Radiol.* **51**, 273–279. (doi:10.1097/RLI.0000000000000273)
82. Saliba W, El-Haddad B. 2009 Secondary hyperparathyroidism: pathophysiology and treatment. *J. Am. Board Fam. Med.* **22**, 574–581. (doi:10.3122/jabfm.2009.05.090026)
83. Bobko AA, Eubank TD, Driesschaert B, Dhimitruka I, Evans J, Mohammad R, Tchekneva EE, Dikov MM, Khramtsov VV. 2017 Interstitial inorganic phosphate as a tumor microenvironment marker for tumor progression. *Sci. Rep.* **7**, 41233. (doi:10.1038/srep41233)
84. Port M, Idée J-M, Medina C, Robic C, Sabatou M, Corot C. 2008 Efficiency, thermodynamic and kinetic stability of marketed gadolinium chelates and their possible clinical consequences: a critical review. *Biometals* **21**, 469–490. (doi:10.1007/s10534-008-9135-x)
85. Elizondo G, Fretz C, Stark D, Rocklage S, Quay S, Worah D, Tsang YM, Chen MC, Ferrucci JT. 1991 Preclinical evaluation of MnDPDP: new paramagnetic hepatobiliary contrast agent for MR imaging. *Radiology* **178**, 73–78. (doi:10.1148/radiology.178.1.1898538)
86. Pan D, Schmieder AH, Wickline SA, Lanza GM. 2011 Manganese-based MRI contrast agents: past, present, and future. *Tetrahedron* **67**, 8431–8444. (doi:10.1016/j.tet.2011.07.076)
87. Zeng L, Luo L, Pan Y, Luo S, Lu G, Wu A. 2015 *In vivo* targeted magnetic resonance imaging and visualized photodynamic therapy in deep-tissue cancers using folic acid-functionalized superparamagnetic-upconversion nanocomposites. *Nanoscale* **7**, 8946–8954. (doi:10.1039/C5NR01932J)
88. Shen Z, Wu A, Chen X. 2017 Iron oxide nanoparticle based contrast agents for magnetic resonance imaging. *Mol. Pharm.* **14**, 1352–1364. (doi:10.1021/acs.molpharmaceut.6b00839)
89. Wang YXJ. 2015 Current status of superparamagnetic iron oxide contrast agents for liver magnetic resonance imaging. *World J. Gastroenterol.* **21**, 13 400–13 402. (doi:10.3748/wjg.v21.i47.13400)
90. Choi J-S, Lee J-H, Shin T-H, Song H-T, Kim EY, Cheon J. 2010 Self-confirming 'AND' logic nanoparticles for fault-free MRI. *J. Am. Chem. Soc.* **132**, 11 015–11 017. (doi:10.1021/ja104503g)
91. Gallo J, Harriss B, Hernández-Gil J, Bañobre-López M, Long N. 2017 Probing $T_1$–$T_2$ interactions and their imaging implications through a thermally responsive nanoprobe. *Nanoscale* **9**, 11 318–11 326. (doi:10.1039/C7NR01733B)
92. Zeng L, Ren W, Zheng J, Cui P, Wu A. 2012 Ultrasmall water-soluble metal–iron oxide nanoparticles as $T_1$-weighted contrast agents for magnetic resonance imaging. *Phys. Chem. Chem. Phys.* **14**, 2631–2636. (doi:10.1039/c2cp23196d)
93. Garcia J, Tang T, Louie AY. 2015 Nanoparticle-based multimodal PET/MRI probes. *Nanomedicine* **10**, 1343–1359. (doi:10.2217/nnm.14.224)
94. Bulte JW, Modo MM. 2017 *Design and applications of nanoparticles in biomedical imaging*. Berlin, Germany: Springer.